



A global model study of processes controlling aerosol size distributions in the Arctic spring and summer

Hannele Korhonen,¹ Kenneth S. Carslaw,¹ Dominick V. Spracklen,¹ David A. Ridley,¹ and Johan Ström²

Received 28 June 2007; revised 7 September 2007; accepted 18 December 2007; published 24 April 2008.

[1] We use a global chemical transport model (CTM) with size-resolved aerosol microphysics to evaluate our understanding of the processes that control Arctic aerosol, focussing on the seasonal changes in the particle size distribution during the transition from Arctic haze in spring to cleaner conditions in summer. This period presents several challenges for a global model simulation because of changes in meteorology, which affect transport pathways and precipitation scavenging rates, changes in the ocean-atmosphere flux of trace gases and particulates associated with sea ice break-up and increased biological activity, and changes in photolysis and oxidation rates which can affect particle nucleation and growth rates. Observations show that these changes result in a transition from an accumulation mode-dominated aerosol in spring to one dominated by Aitken and nucleation mode particles in summer. We find that remote Arctic aerosol size distribution is very sensitive to the model treatment of wet removal. In order to simulate the high accumulation mode concentrations typical of winter and spring it was necessary to substantially reduce the scavenging of these particles during transport. The resulting increases in accumulation mode lead to improvement in the modeled Aitken mode particle concentrations (which fall, due to increased scavenging in the free troposphere) and produce aerosol optical depths in good agreement with observations. The summertime increase in nucleation and Aitken mode particles is consistent with changes in local aerosol nucleation rates driven mainly by increased photochemical production of sulphuric acid vapor and, to a lesser extent, by decreases in the condensation sink as Arctic haze decreases. Alternatively, to explain the observed summertime Aitken mode particle concentrations in terms of ultrafine sea spray particles requires a sea-air flux a factor 5–25 greater than predicted by current wind speed and sea surface temperature dependent flux parameterizations. The enhanced total flux is clearly higher than measured in the Arctic and cannot explain the observed nucleation mode in the high Arctic. The model suggests that the summertime source of Aitken particles has very little effect on the accumulation mode and aerosol optical depth but they may contribute to cloud condensation nuclei in clouds with updraught velocities greater than about 15 cm/s. From a global aerosol modeling perspective, our understanding of Arctic aerosol is poor. We suggest several processes that currently limit our ability to simulate this challenging environment.

Citation: Korhonen, H., K. S. Carslaw, D. V. Spracklen, D. A. Ridley, and J. Ström (2008), A global model study of processes controlling aerosol size distributions in the Arctic spring and summer, *J. Geophys. Res.*, *113*, D08211, doi:10.1029/2007JD009114.

1. Introduction

[2] Climate warming is proceeding faster in the Arctic than in any other region of the world, with IPCC projections predicting a 5°C temperature increase by the end of this century [Christensen *et al.*, 2007]. While radical cuts in anthropogenic greenhouse gas emissions are obviously the most efficient way to slow down the observed and projected

changes in the Arctic climate, Law and Stohl [2007] have suggested that reductions of other anthropogenic pollutants, such as light absorbing black carbon (BC) aerosol, could benefit the Arctic more than regions at lower latitudes. This is because the surface albedo in the Arctic is very high, and multiple reflection and scattering of short wave radiation between the aerosol layer and the surface covered in snow and ice enhances the absorption of solar radiation by BC aerosol. On the other hand, deposition of BC on snow and ice reduces the albedo and thus heats up the surface. Despite a general decreasing trend of anthropogenic pollution to the Arctic throughout the 1980s and 1990s, Quinn *et al.* [2007] have reported that the downward trend in BC

¹School of Earth and Environment, University of Leeds, Leeds, UK.

²Department of Applied Environmental Science, University of Stockholm, Stockholm, Sweden.

concentrations in North American Arctic has stopped and may have reversed in the first half of this decade.

[3] Anthropogenic influence on the Arctic atmosphere is most pronounced in late winter and early spring when, in a phenomenon known as the Arctic haze, high concentrations of aged particles and trace gases enter the Arctic atmosphere and remain for prolonged periods. The winter/spring Arctic aerosol is characterized by a relatively high concentration of accumulation mode particles and very little aerosol in smaller size ranges [Shaw, 1984; Ström *et al.*, 2003; Yamanouchi *et al.*, 2005; Engvall *et al.*, 2007]. The accumulation of pollution in the region is promoted by favorable transport in cold and dry anticyclonic air masses from mainly northern Eurasian sources [Stohl, 2006; Raatz and Shaw, 1984]. In the Arctic frequent strong temperature inversions lead to a stable atmosphere which together with the dryness of the air minimizes cloud formation and precipitation scavenging and thus increases the lifetime of pollutants [Shaw, 1995]. An important component of the Arctic haze is anthropogenic aerosol particles consisting mainly of sulphate and to a minor extent of BC, organic carbon (OC) and nitrate. These long-range transported particles have a considerable effect on the Arctic climate as the natural concentration of cloud condensation nuclei (CCN) in the region is low. Comparisons with measurements from lower latitudes suggest that the microstructure of the clouds in the Arctic is particularly sensitive to anthropogenic pollution [Garrett *et al.*, 2004]. In an analysis of a multiyear measurement data set, Lubin and Vogelmann [2006] found that the first indirect aerosol effect caused by the haze aerosol increases the downward long-wave thermal flux in the region on average by 3.4 W/m^2 , which is comparable to the warming effect from greenhouse gases. However, based on a set of radiative transfer simulations, the same authors suggested that the shortwave manifestation of the first indirect effect, which cools the surface, may be of similar magnitude than the warming effect [Lubin and Vogelmann, 2007]. Climate model studies indicate also that scattering and absorption of radiation by haze aerosol can cause changes in regional circulation and humidity patterns [Rinke *et al.*, 2004].

[4] In summer the anthropogenic influence on the Arctic is much weaker, although episodically present [Iziomon *et al.*, 2006; Xie *et al.*, 2007]. Summertime Arctic aerosol is characterized by high Aitken mode particle concentrations and very low accumulation mode [Ferek *et al.*, 1995; Ström *et al.*, 2003; Heintzenberg *et al.*, 2006; Engvall *et al.*, 2007]. Recent size distribution measurements from Svalbard show a rapid shift from accumulation mode dominated haze aerosol to Aitken mode dominated summer aerosol every year in late May within a window of few weeks [Engvall *et al.*, 2007]. Similarly, measurements at Barrow, Alaska, show a decline in scattering coefficients for submicron aerosol and an increase in Ångström exponent during the spring and early summer [Quinn *et al.*, 2002]. Compared to winter, the air masses arrive to the Arctic basin from cleaner regions, the oceanic sectors being important entry routes, and the transport is also much slower [Stohl, 2006]. Continental influence is most evident during boreal forest fire episodes [Stohl, 2006; Stohl *et al.*, 2006]. The summer atmosphere is characterized by optically thin low lying clouds and fogs which can be present for as much as 90%

of the time and produce frequent drizzle [Curry *et al.*, 1996; Lawson *et al.*, 2001; Intrieri *et al.*, 2002; Tjernström, 2005]. Because of long transport times and enhanced wet removal in low lying clouds and near-surface fogs, local particle sources become important. After the summer in around September, the Arctic aerosol distribution starts to shift toward accumulation mode again but typical particle concentrations remain relatively low until the Arctic haze episodes appear in February/March.

[5] The seasonal changes in aerosol long-range transport and removal mechanisms have a large effect on the mean properties of the aerosol populations in winter and summer. However, previous studies have also suggested that several local factors could be important, including the release of biogenic aerosol precursor gases as the ice melts and increased solar radiation for the oxidation of precursor gases. The retreating sea ice uncovers large areas of open water which provide a source of the aerosol precursor gas dimethylsulphide (DMS). The summertime Arctic Ocean is a strong source of DMS and airborne measurements have shown typical summertime concentration of few tens of pptv with occasional peaks at several hundred pptv [Ferek *et al.*, 1995]. DMS oxidises in the atmosphere to SO_2 which reacts in cloud droplets to form nss-sulphate. On the other hand, further gas phase oxidation of DMS-derived SO_2 to H_2SO_4 is considered the main source of nucleating agents and thus Aitken mode particles in remote marine regions [Raes, 1995; Bates *et al.*, 1998]. Compared to low latitudes, polar regions have an additional source of DMS in spring and summer. In the Arctic and Southern Oceans, high concentrations of DMS and its biological precursor dimethylsulphoniopropionate (DMSP) have been found trapped in and under sea ice [Trevena *et al.*, 2000; Turner *et al.*, 1995; Ferek *et al.*, 1995]. As the sea ice melts, significant concentrations of these sulphur gases can be released into the atmosphere well before phytoplankton bloom periods. Indirect evidence of this has been found by Gabric *et al.* [2005b] whose analysis of satellite data from Southern Ocean showed that over the sea ice zone aerosol optical depth signal reached its peak six weeks before chlorophyll concentration signal in spring. Studies have found correlations between the seasonal cycles of fine particle concentrations and those of particulate MSA^- [Quinn *et al.*, 2002] and atmospheric DMS [Ferek *et al.*, 1995], suggesting that the enhanced Aitken mode in summer can be linked to oceanic release of DMS.

[6] Direct emission of particulates from the sea surface has also been suggested as a source of high concentrations of Aitken mode particles in summer. Late summer measurements of Bigg and Leck [2001] in the high Arctic revealed that, on days with very high small particle concentrations in the boundary layer, particles smaller than 50 nm showed no sign of sulphuric acid. Instead, the particles were nonvolatile and nonhygroscopic implying they consisted of organic matter. These measurements suggest that the dominant Aitken mode particle source in summer may be primary, at least on days when mixing of free troposphere (FT) particles from aloft is inhibited.

[7] In order to predict the future changes in Arctic aerosol distribution and in the radiative effect of the particles, it is important to first understand the factors that control the properties of the Arctic marine boundary layer aerosol in the

present climate. The ongoing warming of the Arctic is likely to alter the sources and microphysical processes of the aerosol population in the region. Transport patterns of anthropogenic pollution may change dramatically if the fast warming of the Arctic weakens the winter time polar dome and thus leads to more efficient pollution transport from industrialised regions at lower latitudes [Law and Stohl, 2007]. Dry summers in the high latitude forested regions can mean more frequent forest fires which are already the main source of BC to the Arctic in summer [Stohl, 2006; Stohl *et al.*, 2006]. The shrinking of the Arctic sea ice cover is predicted to accelerate especially in the biologically active season and could lead to near sea ice free Septembers within 30–50 years [Holland *et al.*, 2006]. Such strong changes in open water surface area would significantly enhance the annual fluxes of primary particles and DMS, the latter of which could increase by as much as 80% by the time of equivalent CO₂ tripling (2080) [Gabric *et al.*, 2005a]. Further changes of DMS flux can be caused by changes in phytoplankton species as the seawater temperature increases.

[8] Large-scale model studies of the source and maintenance of Arctic aerosol are very limited, and no studies have examined the detailed changes in the aerosol size distribution. Nevertheless, previous studies have highlighted the difficulty of simulating long-range transport of aerosol material to the Arctic. Rasch *et al.* [2000], in their comparison of 15 models, reported that only 2 of the models correctly simulated high Pb210 concentrations during the Arctic haze period over Greenland. Two recent general circulation model (GCM) studies have highlighted the difficulty of capturing the aerosol seasonality in the region, with the aerosol concentrations and optical properties often greatly underestimated in the Arctic haze months. Simulations of Generoso *et al.* [2007] using the LMDZ GCM with a bulk (mass only) aerosol scheme predicted monthly mean aerosol optical depth (AOD) up to a factor of 3 lower than observed over Svalbard from April to June. Using satellite data assimilation techniques, it was concluded that the discrepancy was due to underestimating both sulphate and BC transport to the site. Their unconstrained model also produced an incorrect seasonal variation in high Arctic aerosol optical thickness, which tended to increase from spring to summer rather than decrease. Similarly, the Goddard Institute for Space Studies GCM [Koch and Hansen, 2005] predicted springtime peak BC concentrations at Barrow, Alaska, a factor of 3 lower than observed for March and also failed to capture the seasonal variation, although predictions for sulphate were in better agreement with observations. The hemisphere-scale transport model used in the study of Seland and Iversen [1999] under-predicted the winter time BC concentration by approximately one order of magnitude at Alert, Canada, and the sulphate concentration by several factors to over an order of magnitude at Alert and at Bjørnøya (north of Norway). Also this model failed to produce the observed seasonal variation in the Arctic BC concentration.

[9] In this paper, we use observations of aerosol size distribution from the Arctic together with a global size-segregated aerosol microphysics model to evaluate our understanding of the processes that control the Arctic aerosol. Our focus will be on the first half of the year,

i.e., on the Arctic haze period and the spring-to-summer transition. Our objective is to assess the ability of a global aerosol model to capture the important changes in the aerosol properties from spring to summer and to identify gaps in our understanding and weaknesses in current model formulation.

2. Model Description

[10] The global aerosol model GLOMAP is an extension to the TOMCAT 3-D chemical transport model [Chipperfield, 2006; Stockwell and Chipperfield, 1999]. A detailed description of GLOMAP is given by Spracklen *et al.* [2005a]. The model is run with a T42 spectral resolution ($2.8^\circ \times 2.8^\circ$) and with 31 hybrid σ -p levels extending to 10 hPa. Large-scale atmospheric transport is specified from European Centre of Medium-Range Weather Forecasts (ECMWF) analyses at 6-hour intervals. The ECMWF analyses compare well with other global reanalyses in the Arctic and describe the atmospheric transport in the region reliably [Bromwich *et al.*, 2007].

[11] GLOMAP represents the aerosol size distribution with a sectional moving center scheme using 20 size sections to cover the size range of 3 nm to 20 μm . In the runs presented here, the aerosol composition is described with two components: one soluble component representing sulphate and sea spray aerosol, and one totally insoluble component representing primary organic carbon and black carbon aerosol. The masses of both components along with the number of particles are tracked in each size section. The two components are simulated as internally mixed; in other words, the components are assumed to mix instantaneously and therefore even freshly emitted BC/OC particles can act as CCN if the particle distribution contains some soluble material. The soluble component is given the physical properties of sulphate, which leads to a slight underestimation of the average particle size under humid conditions because in reality sea salt is more hygroscopic of the two compounds. The insoluble component has the physical properties of BC. As the primary OC is typically nonhygroscopic [Raymond and Pandis, 2002], the lumping of BC and OC together does not affect the simulated particle wet size significantly.

[12] The aerosol processes in the baseline runs are primary emissions of sulphate, sea spray and OC/BC particles; binary homogeneous nucleation of H₂SO₄ and H₂O according to Kulmala *et al.* [1998]; condensation of H₂SO₄; hygroscopic growth; coagulation; wet and dry deposition; transport; and cloud processing. DMS emissions from the oceans are calculated using monthly mean seawater concentrations from Kettle and Andreae [2000] and the sea-to-air transfer velocity of Nightingale *et al.* [2000]. Anthropogenic SO₂ emissions are from Cofala *et al.* [2005] and volcanic SO₂ emissions based on Andres and Kasgnoc [1998] and Halmer *et al.* [2002]. We assume that 2.5% of SO₂ is emitted as primary sulphate particles at particle sizes proposed by Stier *et al.* [2005]. Primary sea salt emissions are calculated according to Mårtensson *et al.* [2003] for dry particle diameters between 20 nm and 2 μm , and according to Monahan *et al.* [1986] for dry sizes larger than 2 μm . Primary carbonaceous emissions are taken from van der Werf *et al.* [2003] for vegetation fires and from Bond *et al.* [2004] for

fossil and biofuels. BC/OC particles are emitted as lognormal modes at sizes proposed in AEROCOM emissions inventory (<http://nansen.ipsl.jussieu.fr/AEROCOM>).

[13] Sea ice coverage follows monthly mean data taken from British Atmospheric Data Centre (BADC) database. Monthly mean boundary layer clouds are from International Satellite Cloud Climatology Project (ISCCP) archive. Cloud drop activation in these clouds is calculated according to the mechanistic scheme of *Nenes and Seinfeld* [2003] using a random updraught velocity in the range 15–30 cm/s and the activated drops are assumed to grow to 40 times their dry size. Aqueous phase H_2SO_4 forms in these boundary layer clouds through the reaction of SO_2 and H_2O_2 only. Precipitation scavenging of particles and water-soluble gases is considered only for higher level convective and frontal clouds as diagnosed every 6 h in host model TOMCAT separately from ISCCP boundary layer clouds.

[14] For the simulations presented here, the model is spun up for two months (January and February 2001) and comparison with measurements is made for March to July 2001.

3. Observations

[15] The only continuous long-term measurements of aerosol size distributions in the Arctic are available from Zeppelin station in Svalbard (78° 58'N, 11° 53'E, 474 m above sea level). Sitting on an elevated mountain ridge, the station receives hardly any local anthropogenic pollution and is thus well suited to study the effects of long-range transport and local natural aerosol processes. Except very occasionally, the station is located below the boundary layer cloud top and can therefore be taken to represent the conditions in the boundary layer [*Ström et al.*, 2003].

[16] A detailed description of the measurement set-up at Zeppelin station in Svalbard can be found by *Ström et al.* [2003] for aerosol size distribution and from EMEP (Co-operative programme for monitoring and evaluation of the long-range transmission of air pollutants in Europe) data website (<http://www.nilu.no/projects/ccc/emepdata.html>) for gas-phase compounds and precipitation. The particle size distribution is measured over the size range of 20 to 630 nm in diameter with a custom built Hauke type Differential Mobility Analyzer (DMA) coupled to a TSI 3760 Condensation Particle Counter (CPC). Daily gaseous SO_2 concentrations are measured with KOH-impregnated Whatman 40 filter and further analyzed with ion chromatography.

[17] In this study, we compare the model results primarily with monthly averaged measurements from March to July 2001. The monthly averages were calculated from hourly averaged measurements filtered for periods when the station was inside a cloud using the criterion suggested by *Engvall et al.* [2007]: all hourly distributions that had accumulation mode (size range 90–530 nm as defined by *Engvall et al.*) concentration below 35 cm^{-3} were left out of the analysis. This filtering removed 1.3% of size distribution data for

March, 7.1% for April, 15.8% for May, 38.1% for June and 35.1% for July. In general, the size distribution in Svalbard shows two distinct modes: one in the Aitken mode size range (from 20 to ~50–70 nm depending on season) and one in the accumulation mode size range (from ~50–70 to 630 nm). Because of the fairly high lower cut-off size of the size distribution instrument, no clear nucleation mode is detected in the data used in this study. We do not expect our model with a grid box size of $2.8^\circ \times 2.8^\circ$ to capture the exact details of the size distribution at Svalbard; however, the general monthly mean features and the differences between the months are observed throughout the Arctic and should therefore be picked up in the model.

[18] We also use field campaign measurements of aerosol size distributions from the high Arctic. *Heintzenberg et al.* [2006] summarize observations from three summer experiments in the pack ice region (International Arctic Ocean Expeditions (AOE) in 1991, 1996, and 2001) and present multimodal lognormal fits to median particle size distributions under fog and cloud free conditions. For particles larger than 20 nm, the median distributions for all three campaigns have a strikingly similar shape to those in Svalbard averaged over summers 2001–2005, albeit the absolute particle concentrations in the pack ice region are much lower. Because of a lower minimum detection limit during AOE campaigns (3–5 nm depending on the expedition), the high Arctic measurements were able to pick up an additional mode with a median geometric mean diameter of 12 nm. This nucleation mode was present for 65% of the time during the 1991 expedition [*Wiedensohler et al.*, 1996].

4. Results

4.1. General Arctic Conditions in March and June 2001

[19] Figures 1 and 2 show monthly mean sea ice coverage, precipitation, DMS and SO_2 concentrations in the Arctic in March and June 2001. In March, the whole Arctic Ocean is covered in sea ice, apart from Barents Sea which receives warm water from the Gulf Stream. Svalbard is located in the transition region from fast ice and pack ice zone to sea ice edge, and can be influenced by open water sources. The modeled monthly mean precipitation rates in the Arctic are low in accordance with the general observed feature of a dry winter and spring atmosphere. The upper right panel of Figure 1 shows also that the modeled precipitation rates are generally in good agreement with measured values at EMEP sites. For the grid box containing Svalbard, the model predicts a monthly mean precipitation rate that is a factor of 2.5 lower than the measured value at Zeppelin station. It should be noted, however, that precipitation is a highly localized phenomenon and it is difficult to compare the modeled values averaged over $2.8^\circ \times 2.8^\circ$ grid cells against point measurements. The modeled DMS concentration at this time of the year is very low and thus the main sources of SO_2 are anthropogenic. However, the

Figure 1. Monthly mean sea ice cover, precipitation and surface level DMS and SO_2 concentrations in March 2001. Circles in precipitation and SO_2 plots show measured monthly mean values at EMEP sites. The location of Zeppelin station is denoted with a red square in upper right panel. Monthly mean sea ice cover is taken from British Atmospheric Data Center (BADC) database.

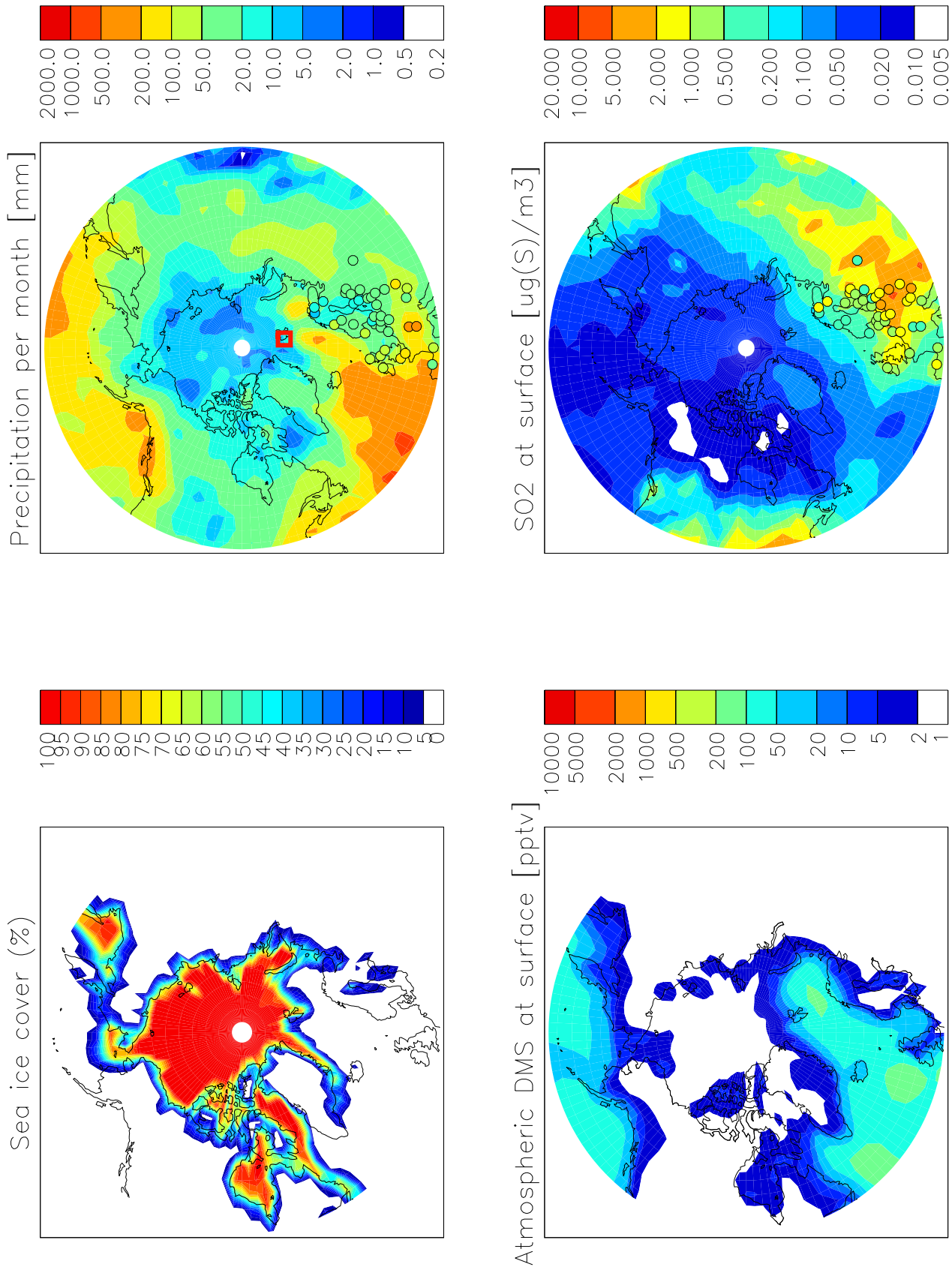


Figure 1

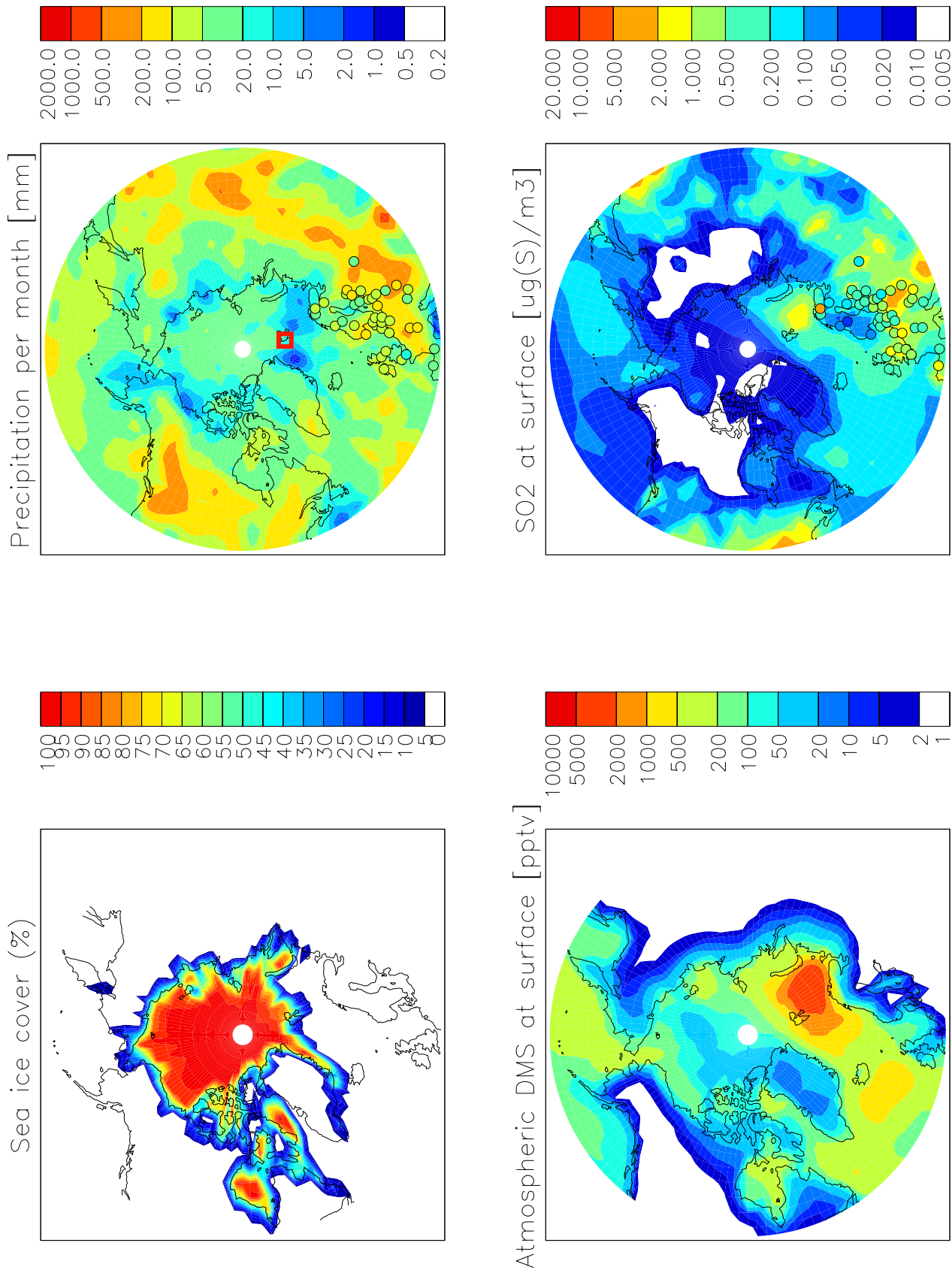


Figure 2

Table 1. Comparison of Modeled and Observed Monthly Mean Particle Concentrations (N_{tot} , in $\#/cm^{-3}$) and Ratios Between Modeled and Observed Total Particle Surface Areas ($A_{\text{mod}}/A_{\text{obs}}$, in Percent) at Zeppelin Station, Svalbard^a

N_{tot} ($\#/cm^{-3}$)	Observation at Svalbard	Model		
		Baseline	$2 \times$ Scav. diameter	BL nucleation
Mar	234	196	267	191
Apr	231	128	142	119
May	209	122	159	135
Jun	440	148	190	294
Jul	407	108	-	-

$A_{\text{mod}}/A_{\text{obs}}$ (%)	Observation at Svalbard	Model		
		Baseline	$2 \times$ Scav. diameter	BL nucleation
Mar	-	16	57	16
Apr	-	13	47	13
May	-	18	67	18
Jun	-	74	128	83
Jul	-	55	-	-

^aObservations from Svalbard are for year 2001. The model simulations presented are (1) baseline simulation (baseline), (2) doubling minimum wet diameter for in-cloud scavenging from 206 nm to 412 nm ($2 \times$ scav. diameter), and (3) including boundary layer nucleation using ‘activation’ mechanism (BL nucleation). The modeled values have been calculated for the particle size range 20–630 nm which is the detection range of the size distribution instrument at Svalbard.

simulated SO_2 concentrations in the Arctic are fairly low. The monthly mean boundary layer concentration at Zeppelin for March is $0.11 \mu\text{g(S)}/\text{m}^3$ compared with measured concentrations of $0.25 \mu\text{g(S)}/\text{m}^3$. The modeled monthly mean at Barrow, Alaska, is 15 pptv ($0.02 \mu\text{g(S)}/\text{m}^3$) which falls into range of measured concentrations (<10 to 60 pptv, i.e., <0.01 to $0.09 \mu\text{g(S)}/\text{m}^3$) reported by *Ferek et al.* [1995] for the lowest 100 m from the surface in April 1992. The underestimation of SO_2 concentration at Svalbard is unlikely to be due to too low SO_2 emissions from anthropogenic sources as the model captures the measured SO_2 concentrations in Europe well (Figure 1, lower right panel). The agreement with measurements is good even at the northern-most EMEP sites, apart from the very high measured concentrations close to Kola Peninsula industrial sources.

[20] In June, the sea ice has started to retreat but in the beginning of the summer still covers the majority of the Arctic Ocean (Figure 2). The modeled precipitation rates are clearly higher than in March and again agree well with EMEP measurements, apart from eastern Central Europe. The measured monthly mean precipitation rate at Zeppelin station is underestimated in June by a factor of about 2. The model predicts a very strong DMS source in the Barents Sea (70° – 80° N, 10° – 40° E) which leads to a high SO_2 concentration in that region. The modeled boundary layer SO_2 concentration in Svalbard is similar in magnitude to that during haze months and agrees well with observations ($0.08 \mu\text{g(S)}/\text{m}^3$ and $0.09 \mu\text{g(S)}/\text{m}^3$, respectively). Modeled

SO_2 values agree well also with measurements from lower latitude European surface sites (Figure 2, lower right panel).

4.2. Comparison of Aerosol Size Distribution Predictions From Baseline Model Simulation With Observations

[21] The set-up of the baseline model simulation was described in section 2. Throughout the simulated period of March to July 2001, the baseline model run greatly underestimates the concentration of 20–630 nm particles compared to measurements at Svalbard (Table 1). The model predicts a decrease in particle number concentration from polluted haze conditions to clean summer conditions whereas the observations show the opposite trend. Therefore the disagreement is particularly strong in June and July. Modeled monthly mean total particle surface areas in spring are only around 15% of those observed, while in summer they are over 50% (Table 1).

[22] Figure 3 shows that the baseline run also fails to capture the features of the measured monthly mean size distributions at Svalbard. Observations show a clear decrease in accumulation mode number and size from spring to summer, and an emerging Aitken mode in May that reaches high concentrations in July. The spring-to-summer transition in the baseline model runs is almost completely opposite: the particle concentration in the accumulation mode increases toward summer and there is no seasonal trend in its size. A significant Aitken mode is present in the model results only in March but not later in summer when it is most pronounced in the observations. The summertime high Arctic observations [*Heintzenberg et al.*, 2006] also have high Aitken and nucleation mode concentrations which the model fails to capture (Figure 4). The model’s spring to summer change in accumulation mode, opposite to that observed, is consistent with the change in aerosol optical thickness predicted by the unconstrained LMDz model of *Generoso et al.* [2007].

[23] The factors leading to such large discrepancies between our model results and the observations are discussed in detail below first for the March haze period and then for summer months.

4.3. Sensitivity of Modeled Aerosol Properties to Particle Wet Scavenging During the Arctic Haze Period

[24] The main discrepancies between the baseline model simulation and the observations at Svalbard during haze months are too low accumulation mode concentrations and too high Aitken mode concentrations in the model. There are microphysical reasons to expect that these two modeled features are linked. In these simulations the Aitken mode in the Arctic boundary layer derives almost entirely from sulphuric acid-water particles nucleated in the cold free troposphere [*Spracklen et al.*, 2005a]. Despite a limited amount of sunlight reaching the Arctic during the haze months, modeled concentrations of SO_2 at 5–7 km altitude are high enough (up to ~ 100 pptv) to sustain sulphuric acid

Figure 2. Monthly mean sea ice cover, precipitation and surface level DMS and SO_2 concentrations in June 2001. Circles in precipitation and SO_2 plots show measured monthly mean values at EMEP sites. The location of Zeppelin station is denoted with a red square in upper right panel. Monthly mean sea ice cover is taken from British Atmospheric Data Center (BADc) database.

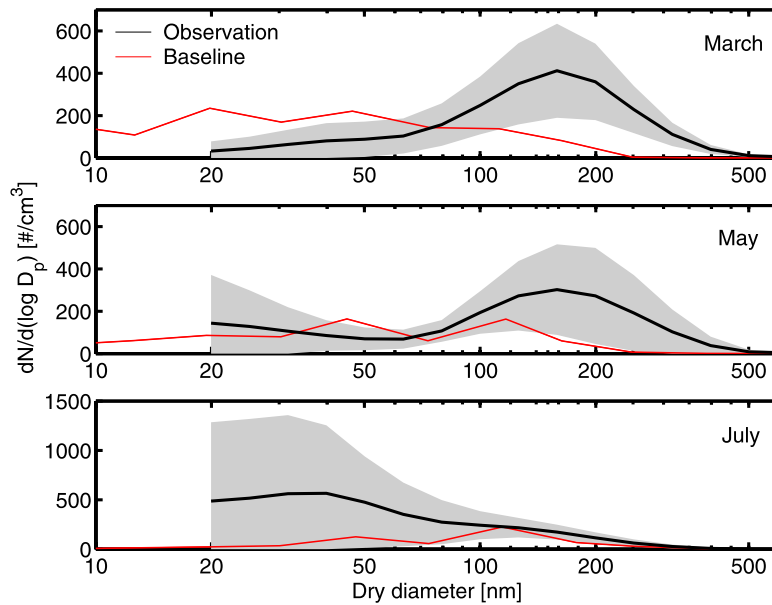


Figure 3. Measured and modeled monthly mean aerosol size distributions at Svalbard in spring and summer 2001. Shaded area indicates the standard deviation of the measured values. Note different vertical scales.

concentration of 0.01–0.03 pptv, sufficient for homogeneous nucleation. As the model predicts much lower than measured particle surface area (13–16% of the measured values in the boundary layer), nucleated particles are not efficiently scavenged by coagulation during their descent toward the boundary layer, which results in a pronounced model Aitken mode at low altitudes. Thus the root cause of differences between the modeled and observed size distributions in spring may be failure to accurately simulate the accumulation mode particle concentration and size.

[25] The large underestimation of the springtime accumulation mode can be caused by underestimating emissions of anthropogenic particulate and gas-phase pollutants, underestimating atmospheric transport rates to the Arctic or overpredicting particle removal mechanisms. *Rotstavn and Lohmann [2002]* have also shown that an underprediction of sulphate (and overprediction of SO_2) at high northern latitudes could be due to the lack of SO_2 oxidation in ice clouds. However, we assume that SO_2 oxidation continues in all low stratiform clouds regardless of temperature and

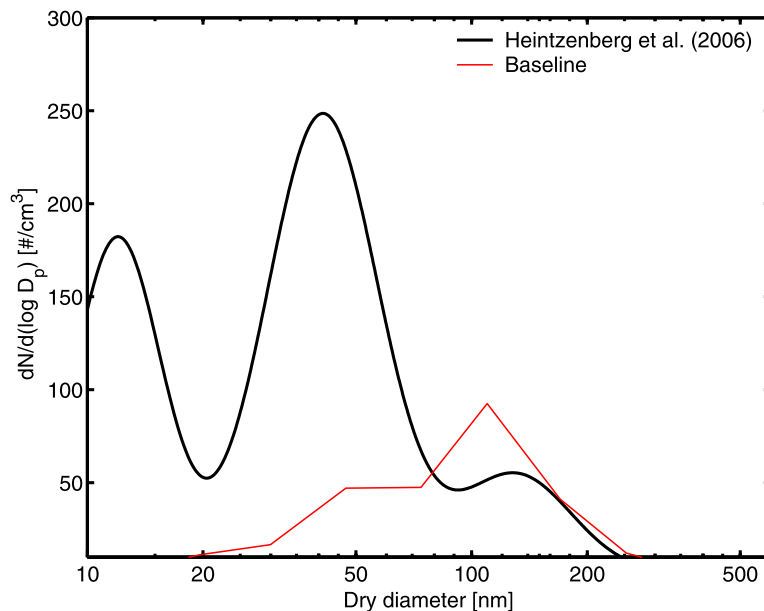


Figure 4. Aerosol size distribution in the summer high Arctic according to lognormal fits based on measurements during AEO expeditions [*Heintzenberg et al., 2006*] and according to baseline simulation for July averaged over latitudes 80° – 90° N and longitudes 31° W– 59° E.

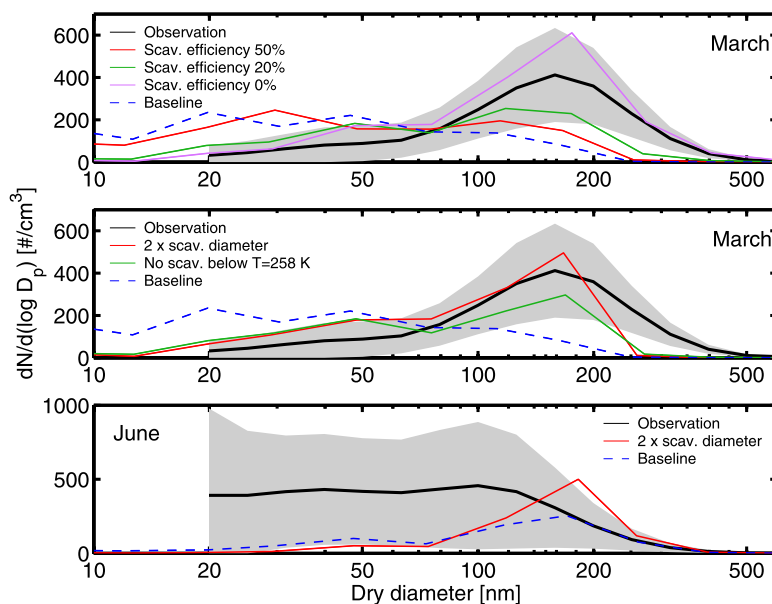


Figure 5. Effect of modified model in-cloud scavenging on the aerosol distribution at Svalbard in March 2001 and in June 2001. Shaded area indicates the standard deviation of the measured values. Note different vertical scales. The model simulations presented are: baseline simulation (baseline), fraction of particles scavenged over a 6-h advection timestep reduced from 99.99% to 0%, 20% or 50% (scav. efficiency 0%; scav. efficiency 20%; scav. efficiency 50%), doubling minimum wet diameter for in-cloud scavenging from 206 nm to 412 nm ($2 \times$ scav. diameter), and not allowing in-cloud scavenging in ice clouds (no scav. below $T = 258$ K).

our model also predicts a reasonable seasonal cycle of SO_2 at high latitudes [Spracklen *et al.*, 2005a]. Over the European and US source regions, $\text{PM}_{2.5}$ in the model generally agrees with observations to within a factor 2 and the modeled SO_2 concentrations agree well with measurements further south, for example over Europe (shown in Figure 1). Therefore incorrect emissions are unlikely to explain the discrepancy in Arctic aerosol mass, which is too low in the model by over an order of magnitude.

[26] Too efficient wet removal of particles during long-range transport is the most likely explanation for the discrepancy in accumulation mode particle concentration and size. As seen in Figure 1, the model captures the dryness of the winter-time Arctic atmosphere and is in fair agreement with precipitation measurements at Svalbard and elsewhere. GLOMAP wet removal rates of SO_2 were presented by Spracklen *et al.* [2005a] and shown to agree well with other global models, although the removal rates have not been compared specifically for transport to the Arctic (nor do measurements exist to evaluate this adequately). On the other hand, the treatment of nucleation scavenging of aerosol in frontal rain clouds, which is the most efficient precipitation removal mechanism of accumulation mode aerosol at high latitudes, is greatly simplified in GLOMAP, as it is in most global models. In grid boxes with rain formation, frontal precipitation is assumed to remove all particles larger than 206 nm in wet diameter over a six-hour advection time step. This diameter is intermediate between the values used by Adams and Seinfeld [2003] and Capaldo *et al.* [1999]. It is larger than the activation diameter of particles in the model clouds (typically 60–100 nm dry size) to account for the fact that only the largest

particles eventually form precipitation sized hydrometeors. In-cloud loss of small activated drops during autoconversion is not taken into account in the model. This might lead to slight overestimation of their concentration when the cloud evaporates. The impaction scavenging of aerosol by rain is treated more physically using a Marshall-Palmer raindrop size distribution and a size-dependent impaction scavenging kernel applied to each aerosol and raindrop size bin.

[27] Figure 5 shows the results of five sensitivity tests in which the nucleation scavenging was altered. In March, decreasing the fraction of particles that are scavenged over a 6-h advection timestep from 99.99% to 50% or to 20% increases the modeled accumulation mode concentration fairly little (Figure 5, top panel). This is because the aerosol originating from Eurasia is likely to pass through several precipitation events during its transport to the Arctic. Middle panel of Figure 5 shows that allowing no nucleation scavenging in ice clouds (assumed to be below 258 K following Chin *et al.* [1996]) improves the agreement with measurements in all size ranges compared to the baseline simulation but the modeled accumulation mode concentration is still lower than measured. Doubling the minimum scavenging diameter to 412 nm (wet particle size), on the other hand, has a very large effect on the simulated distributions (Figure 5, middle panel). The mean size of accumulation mode particles is still underpredicted, but the general features of the distribution and the particle concentration in size range 20–630 nm are much better captured than in the baseline simulation (modeled concentration now 267 cm^{-3} , measured 234 cm^{-3} , see Table 1). However, particle concentrations larger than ~ 200 nm dry diameter

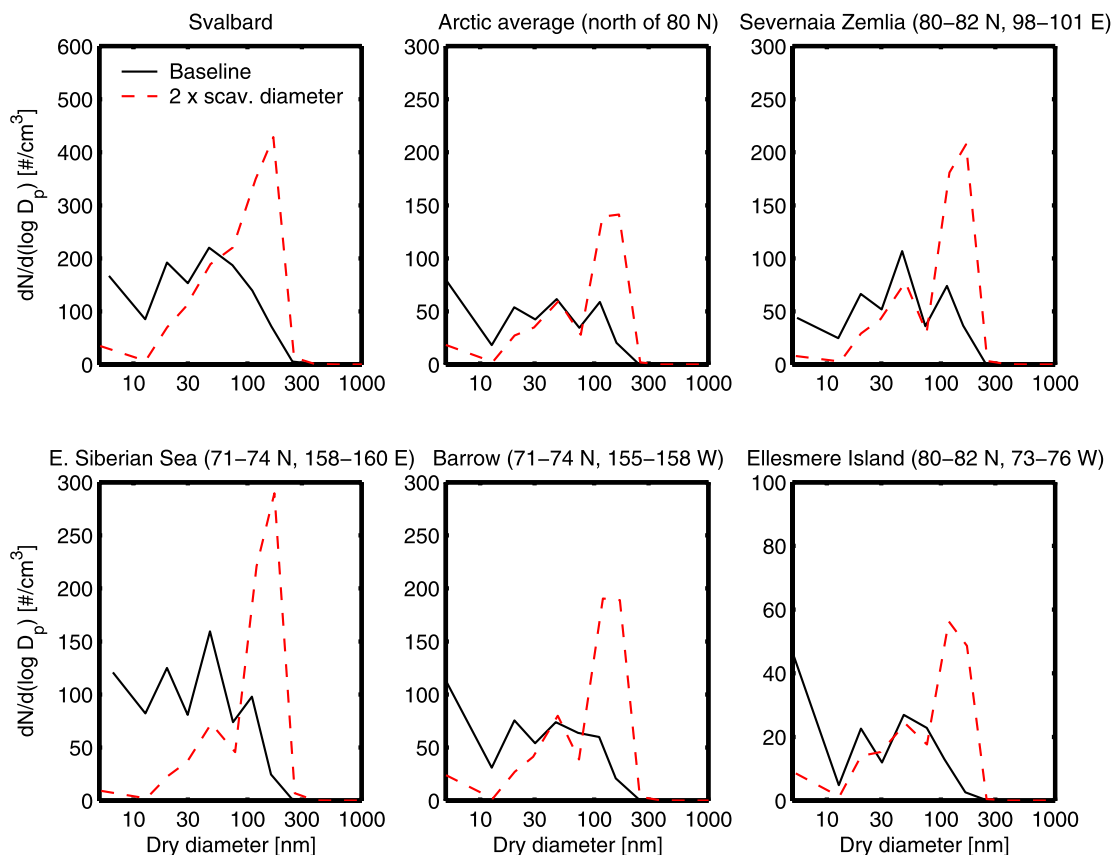


Figure 6. Effect of doubling the in-cloud scavenging diameter at various Arctic sites for March simulation. Note the different vertical scales.

are still underpredicted, suggesting that the largest accumulation mode particles are too strongly removed. This tail of the distribution is well captured if nucleation scavenging in the model is switched off altogether (Figure 5, top panel) but this assumption leads to overprediction of the total accumulation mode particle concentration.

[28] These comparisons cannot be used to decide on the best size-dependent scavenging scheme. Taken together with the findings of other studies [Rasch *et al.*, 2000; Seland and Iversen, 1999; Generoso *et al.*, 2007] they do suggest that scavenging during long-range transport to the Arctic may be overestimated in many global models, although one cannot exclude the possibility that discrepancies in some or all of the earlier studies stem from reasons unrelated to scavenging. An additional difficulty with a model like GLOMAP is that the scavenging affects the size-segregated aerosol distribution and not just the total aerosol mass (like in many other global models). We note that the run with doubled scavenging diameter reduces the aerosol mass at Svalbard by 74% compared to the run without any nucleation scavenging, but still results in an accumulation mode number well within the observed range.

[29] As expected, progressive increases in accumulation mode in the runs with reduced scavenging lead to progressive decreases in Aitken mode concentrations. The total particle surface area in the runs with doubled scavenging diameter is about 4 times higher than in the baseline simulation and leads to Aitken concentrations (20–50 nm diameter) a factor of 2 lower.

[30] The changes in the simulated size distribution as a result of changes in wet removal occur throughout the Arctic (Figure 6) indicating that the changes at Svalbard are representative of the general Arctic. Global size distributions are also affected, though generally to a lesser extent than in the Arctic (Figure 7). Our previous comparison of marine BL size distributions with observation statistics [Spracklen *et al.*, 2007] showed that simulated accumulation mode diameters were typically 15–30% lower and concentrations about a factor 2 higher than observed in polluted northern hemisphere regions. Doubling the in-cloud scavenging diameter improves the comparison of size but worsens the number. This indicates that even if the in-cloud scavenging is underestimated along the transport routes to the winter Arctic, this is probably not the case globally.

[31] Figure 5 (bottom panel) shows that doubling the frontal precipitation nucleation scavenging diameter for the summer runs worsens the comparison with observations, leading to overprediction of the accumulation mode size (by a factor 2) and number. These comparisons suggest that the use of a fixed nucleation scavenging diameter is unlikely to be appropriate for all locations and seasons, although at present we lack the necessary observations and model cloud processes to improve this aspect of the aerosol simulation. Calculating the size of CCN that are removed by nucleation scavenging is a complex cloud physics problem and out of the scope of this study. We note, however, that because of kinetic limitations of droplet growth [Nenes *et al.*, 2001],

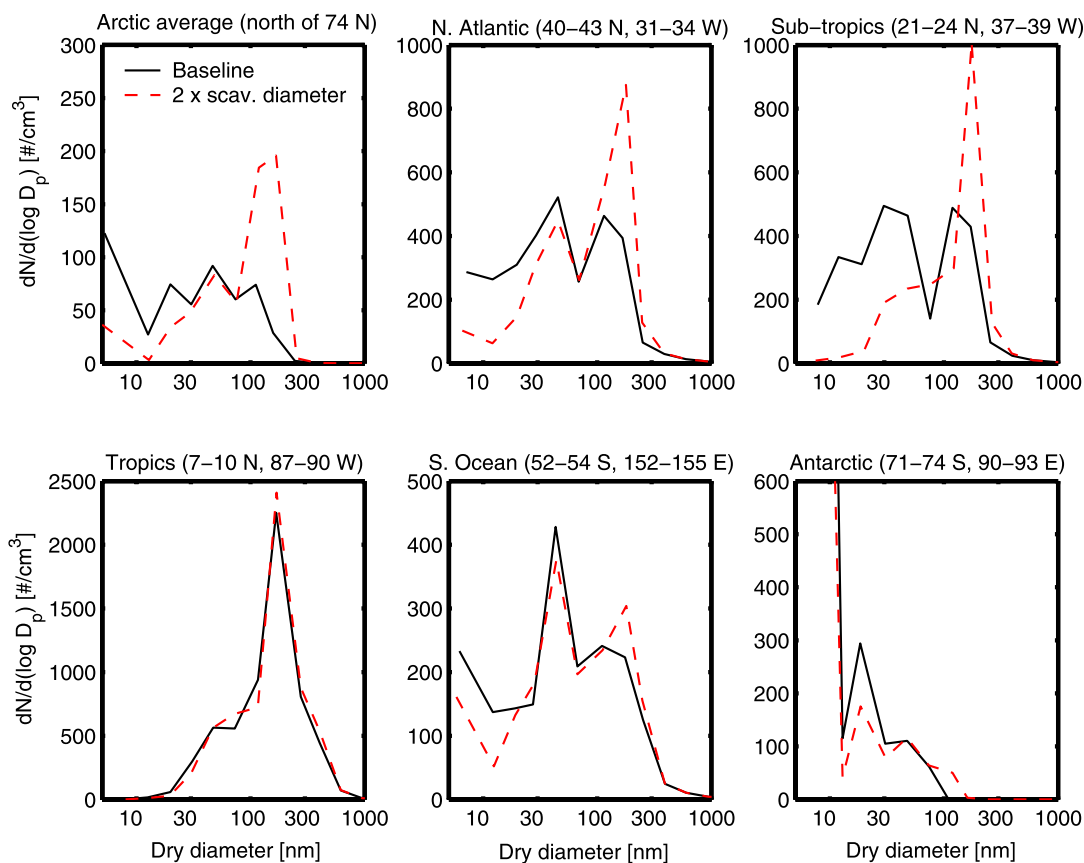


Figure 7. Effect of doubling the in-cloud scavenging diameter at various marine sites for March simulation. Note the different vertical scales.

large changes in the aerosol size distribution seen in the Arctic have a significant impact on the diameter of particles that are activated into cloud drops in updraughts and might therefore be expected to impact scavenging processes. In the

polluted spring environment dominated by accumulation mode aerosol the minimum size of CCN that become cloud droplets is higher than in a clean Aitken mode dominated environment. This is illustrated in Figure 8, which compares

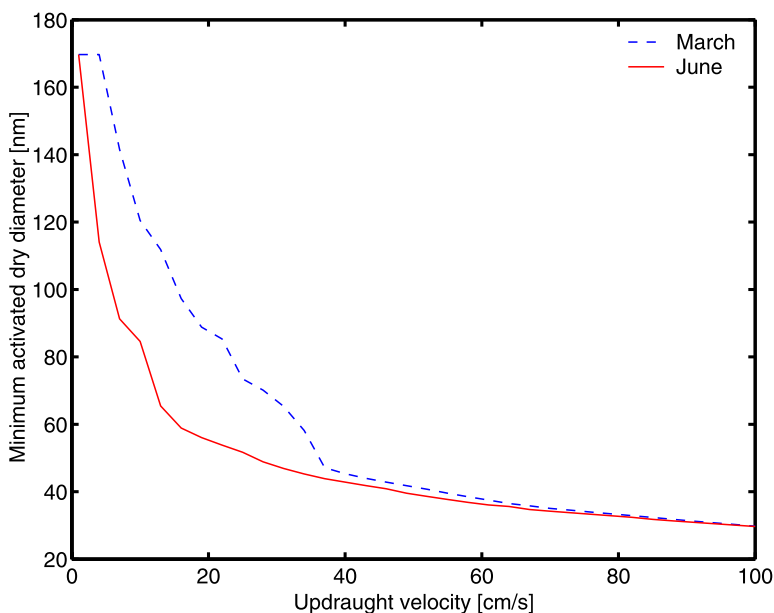


Figure 8. Smallest activated CCN sizes as a function of updraught velocity for March and June using monthly mean size distributions at Svalbard. The activation sizes have been calculated with the scheme of *Nenes and Seinfeld* [2003].

the minimum cloud drop activation diameter at different updraught velocities for monthly mean distributions measured at Svalbard in March and June. The activation diameter was calculated using the mechanistic scheme of *Nenes and Seinfeld* [2003], which is used in the GLOMAP model. For low updraught velocities typical of marine clouds the difference between the polluted and clean conditions is very large. For example, the smallest activated sizes in March and June are 120 nm and 85 nm for updraught of 10 cm/s, 88 nm and 55 nm for 20 cm/s, and 67 nm and 48 nm for 30 cm/s, respectively. Updraught velocities in frontal rainbands are variable but typically around 20–40 cm/s, although may be as high as 100 cm/s in embedded convection. If the characteristics of the monthly mean boundary layer aerosol at Svalbard can be used to approximate the seasonal changes in aerosol size distribution along the transport routes to the Arctic, it is likely that cloud drops that grow large enough to precipitate have been formed on larger CCN during Arctic haze than in clean summer conditions.

[32] We compare the model results from baseline and doubled in-cloud scavenging diameter run also with aerosol optical depth measurements from Arctic AERONET sites (<http://aeronet.gsfc.nasa.gov/>). For the model results AOD is calculated from monthly mean output using the following off-line procedure: Extinction is calculated for each model size section in a grid box and then summed to give AOD in the grid box and further in the column. The Mie factor, which depends on the refractive index and the particle size, is calculated using a look-up table generated from Mie code by G. Thomas (University of Oxford). The combined refractive index is estimated by using the volumetrically averaged refractive indices of the aerosol components. In these off-line AOD calculations we have treated the insoluble model component as BC as the model, as set up here, does not carry BC and OC concentrations separately. Assuming that all insoluble mass is OC decreases the calculated AOD in the Arctic by about 20%.

[33] The changes in Arctic aerosol in the reduced wet scavenging runs have a large impact on the calculated aerosol optical depth and amount of carbonaceous material transported to the region. Top panels of Figure 9 show that the baseline run produces optical depths that are very close to zero, whereas the run with doubled in-cloud scavenging diameter results in AOD values of ~ 0.05 , which is in much better agreement with observations at the Arctic AERONET sites. The calculated increases in AOD between the baseline run and the run with doubled in-cloud scavenging diameter are similar to those in the *Generoso et al.* [2007] model with and without assimilation of satellite AOD measurements, although this does not mean that discrepancies in the study of Generoso et al. are necessarily due to problems with scavenging. The change in scavenging also increases the average mass fraction of carbonaceous aerosol over the Arctic by a factor 4 and by a factor 5 at Svalbard (Figure 9, bottom panels). This change is similar in magnitude to the

underprediction of BC in the models of *Seland and Iversen* [1999], and *Koch and Hansen* [2005] during the Arctic haze. In our model, this increase in mass fraction of carbonaceous aerosol away from continental source areas is due to differences in size distribution of carbonaceous and soluble aerosol mass. Carbonaceous aerosol is emitted at smaller sizes than primary sulphate aerosol, and also a great majority of emitted sea spray mass lies at sizes much larger than OC/BC mass. Compared to the baseline simulation, in which almost all carbonaceous and soluble particles in the accumulation mode are large enough to scavenge before arriving to the Arctic, more carbonaceous than soluble mass in accumulation mode remains unscavenged when in-cloud scavenging diameter is doubled.

[34] These results show that the description of wet scavenging in a global model is critical for an accurate calculation of aerosol transport to the remote Arctic. The impact of errors in scavenging is particularly pronounced at locations remote from midlatitude particle sources [*Rasch et al.*, 2000]. The calculation is particularly problematic when the removal needs to be calculated in a size-dependent way. All previous studies have focused on the aerosol mass transported to the Arctic but, based on observations at Svalbard, 80% of the accumulation mode number accounts for only 30% of the mass. Clearly, more work is needed to improve the wet scavenging in a size-resolved model.

4.4. Boundary Layer Nucleation and Organic Sea Spray Emissions as Potential Aitken Mode Particle Sources During Summer Months

[35] The baseline model simulation underpredicts summertime Aitken mode concentrations (Figure 3) with modeled Aitken concentration decreasing from spring to summer, opposite to the observed trend. In the model, boundary layer Aitken particles originate from sea spray with a peak number emission at 40–60 nm [*Mårtensson et al.*, 2003] and are also mixed down from the FT after nucleating at higher altitudes [*Spracklen et al.*, 2005a]. Modeled FT nucleation occurs at higher altitudes in summer than in spring (driven primarily by higher summer temperatures), which reduces particle concentrations mixed into the boundary layer. The source area of Aitken sea spray particles is slightly larger in the summer as the ice cover retreats, but this does not compensate for the lower particle flux from above, so modeled summer Aitken concentrations are somewhat lower than in spring. *Spracklen et al.* [2005b] previously showed that boundary layer particle concentrations are fairly insensitive to the rate of nucleation in the FT and UT, so this is not an explanation for the underpredicted Aitken mode in summer. Two further possible explanations are (i) a lack of particle nucleation in the lower atmosphere, as has been observed world-wide [*Kulmala et al.*, 2004] and (ii) an underprediction of the sea spray source at Aitken mode sizes.

[36] Several environmental factors, e.g., decreases in sea ice coverage and increases in biological activity, can favor a

Figure 9. Top panels show the simulated aerosol optical depth (AOD) in baseline run (top left) and when in-cloud scavenging diameter is doubled (top right) compared with AOD measured at AERONET sites (circles). Bottom panels show the simulated mass ratio of the insoluble model component (BC and OC) at the surface in baseline run (bottom left) and when in-cloud scavenging diameter is doubled (bottom right).

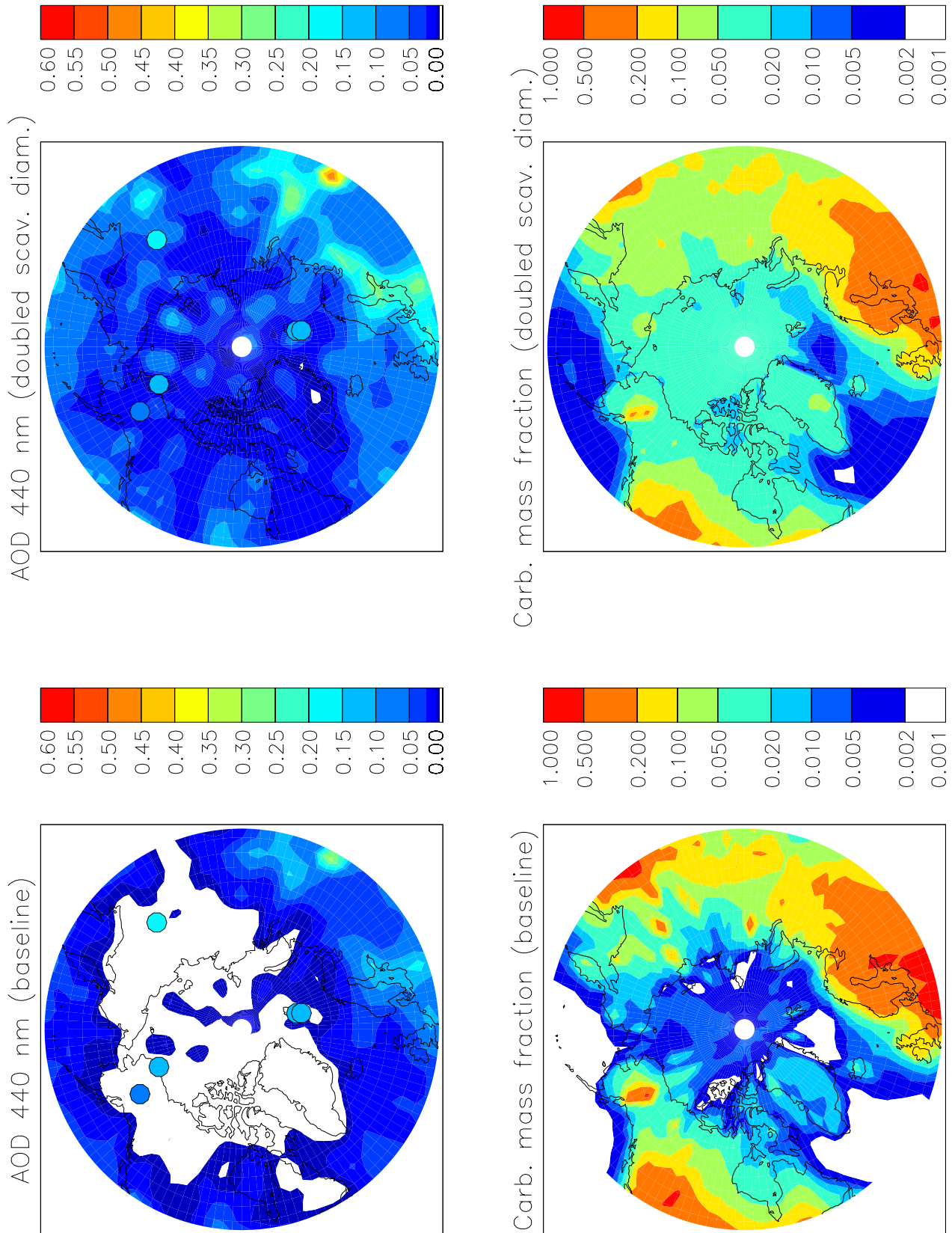


Figure 9

summer-time peak in Arctic particle formation. The retreating sea ice exposes large areas of water to wind stress which results in primary emissions of sea spray and other ocean-derived particles. As the biological activity increases toward summer, the ocean surface layer contains surface active organic species that can be ejected into the atmosphere by bubble bursting [Middlebrook *et al.*, 1998; Tervahattu *et al.*, 2002]. Internally mixed with seawater and its inorganic components, these surfactants can change the surface tension of bubbles and thus modify the size spectrum of aerosol particles. For example Sellegri *et al.* [2006] observed that introduction of synthetic surfactant to artificially generated seawater doubled the flux of Aitken mode sea spray particles at the expense of accumulation mode. Given the large range of organic species present in real seawater and several possible bubble formation mechanisms, the effect of organic surfactants at a specific marine location can be much stronger or much weaker than observed in laboratory studies. Leck and Bigg [2005a] have proposed that bubble bursting can also form Aitken sized particles consisting of secretions of bacteria and microalgae that are free from sea salt. Their single particle analysis suggested that primary emissions of such aggregates may, under some conditions, dominate the ultrafine particle concentrations in Arctic summer, at least in the pack ice region. They suggest that small particles of diameter 20–40 nm can be formed by breakdown of the primary organic aggregates upon exposure to UV radiation and deposition of acidic compounds onto them.

[37] A secondary source of small particles in the Arctic summer is supported by frequent observations of a particle mode below 20 nm over pack ice regions away from primary sources [Wiedensohler *et al.*, 1996; Heintzenberg *et al.*, 2006]. A principal component analysis of Wiedensohler *et al.* [1996] suggested that the observed nucleation mode particles have probably been mixed downward from above or from upper parts of the boundary layer. This possibility is consistent with the observations of Ferek *et al.* [1995] who reported rapid new particle formation at 0.5–2 km altitudes in the spring Arctic in regions where accumulation mode particles were scavenged e.g., by low stratus clouds, which are almost always present in the region in late spring and summer. The most likely source of nucleating vapours during the spring-to-summer transition is DMS produced by ice algae and open water phytoplankton and Ferek *et al.* [1995] reported seawater DMS concentrations in the Arctic comparable to other oceanic regions. Once released into the atmosphere, the DMS is oxidised by OH radicals that are abundant in the Arctic only during summer months. Oxidation products of DMS react in turn to form sulphuric acid, which is currently considered to play a key role in atmospheric nucleation [Kulmala *et al.*, 2004, 2006].

[38] In the following we investigate whether these two hypotheses, i.e., enhanced summer-time primary particle emissions from the oceans and nucleation in or just above the boundary layer, can explain the observed summer time peak in the Aitken mode concentration. We use the baseline model wet scavenging.

4.4.1. Effect of Enhanced Sea Spray Emissions

[39] In the baseline simulation primary emissions from oceans are calculated according to the parameterization of Mårtensson *et al.* [2003], which is based on laboratory

experiments on synthetic seawater. Therefore the parameterization does not take into account any effects that surface-active organic compounds in seawater or primary emissions of microorganism aggregates may have on the size distribution of emitted particles. As the current understanding of these effects is qualitative rather than quantitative, we have conducted a sensitivity test to estimate how strong the effect of organic compounds on the primary particle flux needs to be to sustain the observed Aitken mode number concentrations.

[40] We model the organic particle emissions from bubble bursting by assuming that the shape of the emitted particle size distribution follows that of the Mårtensson *et al.* [2003] sea spray emission flux for particles smaller than 70 nm. The magnitude of the particle flux is then increased until the modeled Aitken mode concentration is of similar magnitude to that observed. This approach assumes that the additional flux is wind speed dependent which might not be the case if the bubble bursting were caused by biological processes as suggested by Leck and Bigg [2005a]. The particles from this additional source are treated as non-hygroscopic and insoluble but are assumed to be mixed with the water-soluble sea spray particles, which we continue to emit according to the original parameterization. The solubility assumption affects the cloud activation of the emitted particles and thus their transfer from Aitken to accumulation mode. As the simulated flux of insoluble particles is much higher than that of soluble sea spray particles, we are likely to underestimate the water solubility of an average internally mixed particle and thus also underestimate the transfer to accumulation mode through cloud processing. Our assumptions therefore enable us to estimate the minimum flux, additional to basic sea spray flux, which is needed to maintain the observed Aitken mode concentration. We do not attempt to model the progressive breakdown of larger primary particles by UV radiation and acidification as suggested by Leck and Bigg [2005a, 2005b], but discuss their potential effects on our results below.

[41] Top panel of Figure 10 compares the model and observations at Zeppelin, Svalbard, in the summer assuming an ultrafine sea spray flux of particles [Mårtensson *et al.*, 2003] increased by a factor of 25 (i.e., 26 times the original flux). It is highly unlikely that the sole effect of organic surfactants could enhance the flux of sea spray particles this much. For example the laboratory experiments of organic surfactants by Sellegri *et al.* [2006] show an increase in Aitken mode concentration of a factor of only 2. Furthermore, the predicted additional particle flux over open water at mean modeled wind speed for the Arctic (5.6 m/s at sea surface, from which calculated 10 m wind speed is 4.6 m/s) is $2.3 \times 10^6 \text{ m}^{-2}\text{s}^{-1}$, which is over an order of magnitude higher than the total particle flux measured over open water in the Arctic [Nilsson *et al.*, 2001]. On the other hand, if the organic matter were to become externally mixed from sea salt and to undergo several fragmentation steps in the atmosphere, as proposed by Leck and Bigg [2005a] for the pack ice region, a much smaller additional flux of particles could lead to high Aitken mode concentrations. According to Leck and Bigg [2005b], an average organic aggregate of around 60 nm emitted from seawater could break down into approximately 8 smaller aggregates of

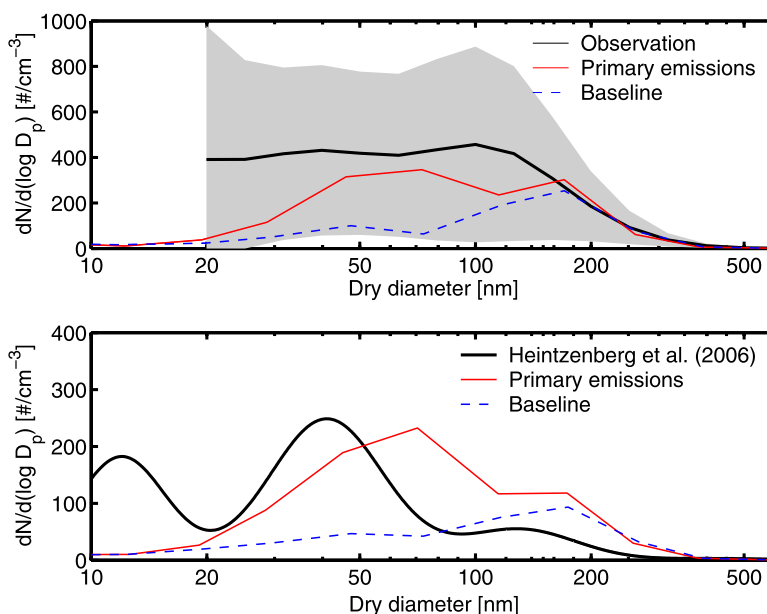


Figure 10. Effect of increased ultrafine primary particle flux ($26 \times$ flux of *Mårtensson et al.* [2003] for particles smaller than 70 nm) in June 2001 at Svalbard (top panel) and at high Arctic averaged over latitudes 80° – 90° N and longitudes 31° W– 59° E (bottom panel).

30 nm, the mid-size of airborne aggregates. If these measurements can be extrapolated to Svalbard latitudes, this would mean that the summertime ultrafine particle flux in the Arctic would need to be approximately 5–6 times that predicted by the *Mårtensson et al.* [2003] parameterization. While such an enhancement in the particle flux is not totally unrealistic, it should be remembered that the hypothesized mechanism of airborne aggregate formation is currently poorly understood and not experimentally confirmed.

[42] Increasing the primary ultrafine particle flux by a factor of 25 does not significantly improve the agreement between the simulated and measured summer distributions in the high Arctic (Figure 10, bottom panel). The emitted particles are much larger in size than the observed Aitken mode, which could be explained by the break down of primary aggregates in the atmosphere as discussed above. However, the observed particle mode at around 12 nm is unlikely to form through this mechanism and points to secondary formation of new particles in the atmosphere.

4.4.2. Effect of Boundary Layer Nucleation

[43] The only nucleation mechanism included in our baseline simulations is the binary scheme of sulphuric acid and water [*Kulmala et al.*, 1998], which forms particles only in very cold conditions, i.e., in practice in the model free troposphere. These particles grow by coagulation and condensation of further sulphuric acid as they are transported down to the boundary layer. We have previously shown that new particle formation in the FT according to this mechanism can explain the concentration and vertical profiles of ultrafine particles in marine background regions over the Pacific, Atlantic and Indian Oceans and can contribute to Aitken particle concentrations in the marine boundary layer [*Spracklen et al.*, 2005a, 2007]. However, according to Figure 3 their contribution to summertime Aitken concen-

trations in the Arctic is small. Observations from around the world, especially from continental sites, have shown that new particle formation frequently takes place also in the planetary boundary layer [*Kulmala et al.*, 2004]. Analysis of these events has shown that particle formation rates depend on the sulphuric acid concentration to the power between 1 and 2 [*Weber et al.*, 1996; *Fiedler et al.*, 2005; *Sihto et al.*, 2006].

[44] For our set of simulations with boundary layer nucleation we have assumed that the nucleation rate of stable clusters (J_{nuc}) depends linearly on the concentration of sulphuric acid, i.e.

$$J_{nuc} = k[\text{H}_2\text{SO}_4]. \quad (1)$$

[45] This mechanism can be interpreted as activation of single sulphuric acid molecules, and *Spracklen et al.* [2006] have shown that it can predict the observed boundary layer events and the resulting particle number concentrations well at a boreal forest site. We restrict this activation mechanism to the boundary layer and assume that new particles higher in the atmosphere form through the binary mechanism.

[46] The rate constant k in equation (1) is taken to be $2 \times 10^{-6} \text{ s}^{-1}$ based on the empirical analysis of *Sihto et al.* [2006]. It should be noted that this value has been deduced from springtime particle formation measurements at a forested continental site and may depend on environmental factors such as temperature, humidity and concentration of organic species. These dependencies are not, however, currently understood and while the chosen value of k may not be fully representative of the high latitude spring and summer conditions, we present it here as a sensitivity study.

[47] Instead of using directly equation (1), which would require extending the simulated particle size range to below 1 nm, we calculate the formation rate of 3 nm particles (J_3)

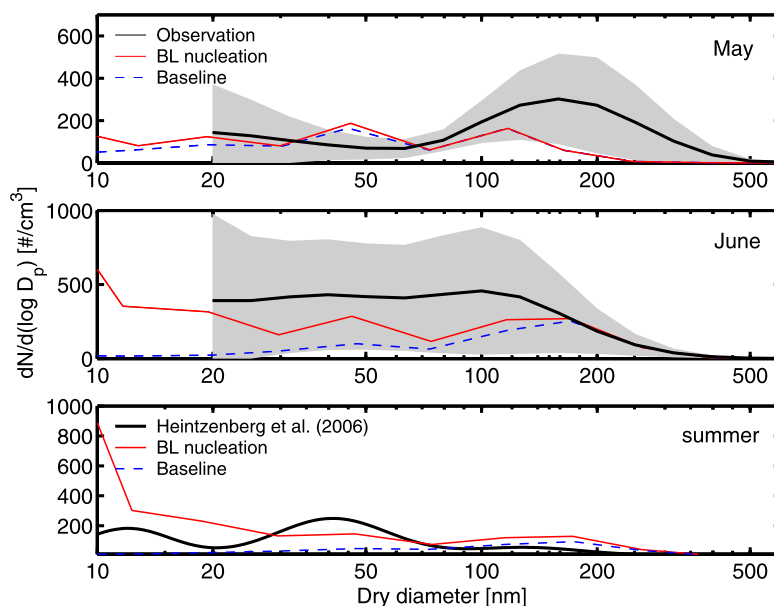


Figure 11. Effect of BL nucleation on the simulated particle size distribution at Svalbard in May and June (top and middle panels), and at high Arctic (80° – 90° N, 31° W– 59° E) in June (bottom panel).

according to the parameterisation of *Kerminen and Kulmala* [2002]. This formation rate is given by

$$J_3 = J_{nuc} \times \exp(-2.11d6 \times CS' / [H_2SO_4]), \quad (2)$$

where CS' is the condensation sink of molecules to the pre-existing particles (given in m^{-2}), $[H_2SO_4]$ is sulphuric acid concentration (given in cm^{-3}) and J_{nuc} is the formation rate of new atmospheric clusters according to equation (1). This parameterisation assumes that the newly formed clusters grow from 0.8 to 3 nm due to condensation of H_2SO_4 and takes into account their coagulation scavenging to the background aerosol.

[48] Emissions of organic vapours from vegetation are thought to contribute significantly to the growth of nucleation mode particles in the boundary layer over the continents [*Birmili et al.*, 2003; *Boy et al.*, 2005]. Vegetation and therefore local emissions of condensable organics in the Arctic are scarce even in summer but some of the gas-phase organic species from lower latitudes can be transported for several days in the atmosphere [*de Gouw et al.*, 2005] and indications of long-lived organic aerosol precursor gases have been observed also in the Arctic [*Kawamura et al.*, 2005]. We include therefore in our simulations a simplified scheme to describe the formation of condensable organic species in the atmosphere. We assume that a fixed fraction of 13% of monoterpene oxidation products forms condensable vapours which are lumped in the model into one non-volatile organic compound. Monthly averaged emissions of monoterpenes are taken from GEIA emission inventory [*Guenther et al.*, 1995]. A more detailed description of the treatment of organics species in the model is given by *Spracklen et al.* [2006].

[49] Introduction of the boundary layer nucleation mechanism adds considerably to the Aitken mode particle population in summer months (Figure 11, top and middle panels) and improves agreement with measured particle

total concentration (Table 1). Particle concentrations between 20 and 50 nm diameter increase by about a factor 3 but are still slightly lower than those observed. The model now captures the spring-to-summer transition from accumulation mode dominated to Aitken mode dominated size distribution fairly well. In May and earlier months the impact of the additional nucleation mechanism is negligible but it has a substantial effect in June. From March to May the modeled H_2SO_4 concentration in the Arctic region is $\sim 10^4$ – 10^5 cm^{-3} , which is too low to form a significant number of particles, but in June H_2SO_4 concentrations are $\sim 10^6$ cm^{-3} and are sufficient to sustain the nucleation and growth of particles to Aitken sizes. It should be noted, however, that the modeled SO_2 concentrations at Svalbard during spring months are an underestimate of the observed values, the discrepancy being largest in April and May when the modeled concentrations are off by approximately an order of magnitude (whereas in June they are in good agreement with measurements). As discussed earlier in the context of Arctic haze, this discrepancy in the model can be caused by problems with anthropogenic SO_2 transport or later in spring by emissions of DMS from melting sea ice which are not simulated in the model. The tendency of the model to underestimate SO_2 concentrations in the spring months is unlikely to have a large effect on the predicted BL nucleation rates during Arctic haze when OH concentrations are very low and accumulation mode aerosol scavenges small nucleated particles efficiently. In May, however, we expect the too low SO_2 concentration in the model to lead to underestimation of H_2SO_4 production rates and thus of BL nucleation rates.

[50] We use therefore off-line calculations based on measured SO_2 concentrations and particle size distributions to study whether the BL nucleation mechanism is able to explain the observed May-to-June shift in the Arctic aerosol properties. The measured monthly mean SO_2 concentrations in May and June are in most years very close to each other

and almost in all years within a factor 3. On the other hand, the model monthly mean OH concentration in the Arctic increases by almost a factor of 3 between the two months, which means that the average production rate of H₂SO₄ increases from May to June. At the same time the condensation sink (CS) decreases by 10% reducing the scavenging of H₂SO₄ molecules and nucleated particles. We use these trends together with equation (2) to estimate the typical formation rates of 3 nm particles (J_3) for these two months. J_3 gives a better approximation than J_{nuc} of the magnitude of new particle flux affecting the Aitken mode concentrations as the coagulation loss rates for particles that have grown beyond 3 nm sizes are approximately an order of magnitude lower than for clusters around 1 nm. By using CS values calculated from measured monthly mean size distributions and a conservative estimate that the H₂SO₄ concentration increases by 50% from $8.7 \times 10^5 \text{ cm}^{-3}$ in May to $1.3 \times 10^6 \text{ cm}^{-3}$ in June (which is the modeled mean value in June when SO₂ concentration is well predicted), we find that the apparent nucleation rate increases by a factor ~ 550 from May to June. This supports the hypothesis that the spring-to-summer shift in the particle distribution can be driven by BL new particle formation. In our calculations the assumed 50% increase in H₂SO₄ concentration alone leads to a factor of 200 increase in the apparent nucleation rate, mainly by affecting the new particle growth rates and thus reducing their scavenging before they reach 3 nm. It should be noted, however, that this increase factor depends on the absolute H₂SO₄ concentrations used in the calculations. The 10% decrease in the condensation sink alone causes a factor of 3 increase in the apparent nucleation rate.

[51] By including BL nucleation mechanism into the model, the agreement with measurements in the high Arctic is slightly improved, especially in the Aitken mode size range (Figure 11, bottom panel). The accumulation mode concentration is predicted to be higher than in the baseline simulation and is therefore too high compared to observations. The model predicts a nucleation mode at around the correct size but the simulated concentration is approximately a factor 5 higher than observed. Similar very high nucleation mode concentrations are predicted throughout the Arctic. High resolution simulations that take account of the particular boundary layer structure, deposition processes and scavenging in fog would be needed to refine our understanding of the role of nucleation in the Arctic boundary layer.

[52] The introduction of a strong local source of nucleation mode particles in the model has a substantial effect on Aitken mode concentrations (primarily through condensation growth and coagulation) but a relatively small effect on the accumulation mode. The accumulation mode number can increase due to the fact that some Aitken mode particles are activated in low level clouds and eventually grow by aqueous SO₂ oxidation to H₂SO₄. In June, the modeled accumulation mode concentration (>100 nm dry diameter) increases by 17% over the Arctic on average (16% at Svalbard), the effect being largest for the lowest size range of the mode. The net impact on Arctic mean AOD is therefore only 3% when the boundary layer nucleation mechanism is introduced, showing that this process is unlikely to be important for the direct radiative properties of Arctic aerosol. The impact on cloud drop number, and

hence cloud reflectivity, depends on how frequently the additional Aitken particles act as cloud condensation nuclei. Figure 8 shows that, in summer, sulphuric acid particles smaller than 60 nm dry diameter will serve as CCN when cloud updraughts exceed $\sim 15 \text{ cm/s}$. Such vertical velocities are frequently observed in summer Arctic BL clouds [e.g., Lawson *et al.*, 2001].

5. Conclusions

[53] We have used an offline global aerosol microphysics and chemistry model to study the processes that control Arctic aerosol. To our knowledge, this is the first attempt to simulate changes in the particle size distribution that occur during spring and summer. Previous large scale model studies have highlighted the difficulty of simulating the long range transport of aerosol material to the Arctic region during winter and spring [Rasch *et al.*, 2000; Seland and Iversen, 1999; Rotstavn and Lohmann, 2002; Koch and Hansen, 2005; Generoso *et al.*, 2007]. These studies have focused on the transport of aerosol mass (either sulphate, black carbon or both). Our model differs from these previous studies in that it simulates the full aerosol size distribution from 3 nm to 20 μm . This enables us to explore the processes that control the well documented large changes in the Arctic aerosol size distribution from spring to summer [Engvall *et al.*, 2007; Quinn *et al.*, 2002, 2007].

[54] In common with the previous studies, our model tends to have too little aerosol mass in the Arctic during the winter-spring haze period. This is manifested as a significant (factor of 4) underprediction of accumulation mode number concentration compared to long-term observations at Svalbard [Engvall *et al.*, 2007] and a very low aerosol optical depth (~ 0 compared with AERONET observed values of ~ 0.05). The uncertainties in the accumulation mode aerosol properties in the more southerly latitude source regions are quite small compared to the very large model-observation difference in the Arctic, suggesting that the problem lies with transport and removal. The most likely cause of this underprediction is the excessive wet removal of aerosol during long-range transport. Previous studies using the same host chemical transport model (TOMCAT) have not revealed any major global discrepancy in wet deposition [Giannakopoulos *et al.*, 1999; Rasch *et al.*, 2000], but the Arctic appears to present a particularly severe test of the model wet removal scheme because it is remote from strong aerosol sources so aerosol abundance becomes dominated by removal processes. Bowling and Shaw [1992] discussed the difficulty of reconciling basic thermodynamic changes in air transported to the Arctic with the survival of air pollutants. They showed that the observed temperature and humidity of polluted Arctic air could only be explained if precipitation occurred during transport or if pollutants were injected high into dry layers at source. They further estimated from measured sulphate aerosol mass scavenging rates (kg SO₄ lost per kg precipitation formation) that up to one-third of the SO₄ aerosol mass would remain after transport. We have shown here that to understand the Arctic aerosol size distribution in springtime requires a refined understanding of how different sized particles are scavenged, and not just how the mass is depleted. A further possibility, not explored here, is that

the problem lies with the meteorological fields used to drive the chemical transport model. Further work will be needed to quantify how accurately a fairly low resolution Eulerian global model can simulate the known transport pathways from Eurasia to the Arctic [e.g., *Stohl*, 2006]. *Bromwich et al.* [2007] studied the reliability of several global reanalyses (including ECMWF) and found that they all produce similar tracking of cyclones in the Arctic, which suggests that atmospheric transport in this region is adequately represented by ECMWF winds.

[55] A number of sensitivity tests showed that the accumulation mode abundance observed at Svalbard during spring could be simulated by reducing nucleation scavenging in clouds practically to zero. This was achieved either by limiting nucleation scavenging to aerosol particles with diameters larger than 400 nm or by switching the process off altogether. However, a similar approach made the model-observation comparison much worse in summer, suggesting that wet removal rates of different sized particles may vary seasonally. The increased accumulation mode abundance in the reduced scavenging runs had a knock-on effect on the simulated Aitken mode, which tended to be overestimated in the control run. Aitken mode concentrations fell by about a factor 2 in the runs with more accumulation mode, which we explain by the increased coagulation scavenging of nucleation and small Aitken mode particles by the accumulation mode during transport.

[56] Wet scavenging of particles in a size-resolving model like GLOMAP presents new challenges that were not an issue in models that simulated only aerosol mass. Most models apply some kind of mass scavenging coefficient. However, most of the accumulation mode number is at small sizes of ~100–200 nm diameter but most of the mass is at larger sizes. The calculation of size-dependent nucleation scavenging rates is much more challenging than for impaction scavenging (rainout), for which an approximate raindrop and aerosol size distribution can be used, and rainout doesn't significantly affect accumulation mode particles which are most important for climate. To account for the fact that rain tends to form from the largest droplets, we have assumed that nucleation scavenging acts on aerosol particles larger than 200 nm diameter (400 nm in the sensitivity test), while particles larger than ~60–100 nm are typically activated into cloud droplets. Clearly this is a crude assumption that needs to be improved. The activation diameter varies substantially with the aerosol size distribution and cloud updraught velocity. The size dependent scavenging rates will depend on these and other processes occurring at the cloud scale.

[57] The summertime Arctic aerosol is dominated by the appearance of Aitken and nucleation mode particles and a reduced size and number of accumulation mode. Our results suggest that the Aitken particles do not form by homogeneous nucleation of sulphuric acid-water particles in the free troposphere. Rather, there needs to be an additional source of nucleation mode particles in or just above the boundary layer [e.g., *Ferek et al.*, 1995; *Wiedensohler et al.*, 1996; *Garrett et al.*, 2002]. We explore two possibilities suggested by previous studies: nucleation of new particles [*Wiedensohler et al.*, 1996; *Quinn et al.*, 2002; *Engvall et al.*, 2007] and a strong source of ultrafine particles from the sea surface [*Leck and Bigg*, 2005a, 2005b]. When we include boundary layer

nucleation at a rate that depends linearly on the sulphuric acid vapor concentration, the model is able to capture the appearance of nucleation and Aitken mode particles in the summer. Off-line calculations indicate that this summertime increase is driven mainly by increases in OH concentration and thus in gas phase H₂SO₄. However, clear model-observation differences remain. For example, the model Aitken mode agrees well with summertime observations at Svalbard [*Engvall et al.*, 2007] and over the pack ice [*Heintzenberg et al.*, 2006] but tends to overpredict nucleation mode concentrations where these have been observed.

[58] Alternatively, to obtain reasonable quantitative agreement with the observed Aitken mode concentrations at Svalbard in June requires an additional ultrafine sea surface source flux a factor 25 higher than measured in laboratory experiments of *Mårtensson et al.* [2003]. In the simulation with enhanced sea spray emissions the total particle flux is over an order of magnitude higher than has been measured in the Arctic [*Nilsson et al.*, 2001]. A significantly lower, but still 5–6 times enhanced, primary flux from sea surface is required if the emitted particles undergo several break-down steps in the atmosphere as proposed by *Leck and Bigg* [2005a, 2005b].

[59] The effect of the Aitken particles on climate is an important open question because their abundance and size are likely to be affected by the warming climate, e.g., through possibly substantial changes in DMS emissions [*Gabric et al.*, 2005a]. We showed that variations in the springtime accumulation mode significantly affected the Aitken mode but, conversely, that large changes in the summertime Aitken mode have a relatively small effect on the accumulation mode. The impact on Aitken mode particles on summer AOD is small, only about 3% increase when boundary layer nucleation is added to the model. The effect of Aitken mode on cloud condensation nuclei depends on the cloud-scale updraught velocity. Based simply on the observed particle size distribution in summer, a realistic updraught velocity of ~15 cm/s would be needed to activate the largest Aitken mode particles of 60 nm dry diameter.

[60] Our model study highlights the need for more experimental data combined with detailed model analyses in order to improve our understanding of the processes controlling the Arctic aerosol. Further work on aerosol-cloud interactions is one of the biggest priorities as clouds not only control the amount of anthropogenic aerosol transported to the region during Arctic haze but also play an important role in the aging of the particles and in facilitating new particle formation in the summer BL by reducing condensation sink. Although remote observations of cloud and aerosols exist together with concurrent (mostly campaign-wise) ground based and airborne measurements, we currently lack a comprehensive data set covering all seasons and all aerosol types characteristic to the Arctic region. Regarding the source of summertime Aitken mode particles, measurement data of sulphuric acid concentrations, VOC emissions from the ocean, as well as aerosol size distributions extended to nucleation mode size range would be highly beneficial to test the BL nucleation hypothesis. Further model-observation studies at high spatial resolution, resolving cloud-scale humidity variations and scavenging of nucleation mode particles in low level summer fogs would also help to advance our understanding of nucleation in the

Arctic marine boundary layer. Size segregated particle flux measurements over the Arctic ocean together with chemical analyses of Aitken mode particles would give information about the effect of organic matter on primary sea spray flux.

[61] **Acknowledgments.** This work was supported by UK Natural Environment Research Council, a Royal Society International Joint Project grant, and the Kone Foundation. Aerosol observations at the Zeppelin station are supported by the Swedish Environmental Protection Agency. We thank B. Holben, J. Hollingsworth, M. Panchenko, R. Wagener and their staff for establishing and maintaining the five AERONET sites used in this study.

References

- Adams, P., and J. Seinfeld (2003), Disproportionate impact of particulate emissions on global cloud condensation nuclei concentrations, *Geophys. Res. Lett.*, *30*(5), 1239, doi:10.1029/2002GL016303.
- Andres, R., and A. Kasgnoc (1998), A time-averaged inventory of sub-aerial volcanic sulfur emissions, *J. Geophys. Res.*, *103*(D19), 25,251–25,261.
- Bates, T. S., V. N. Kapustin, P. K. Quinn, D. S. Covert, D. J. Coffman, C. Mari, P. A. Durkee, W. J. De Bruyn, and E. S. Saltzman (1998), Processes controlling the distribution of aerosol particles in the lower marine boundary layer during the first Aerosol Characterization Experiment (ACE 1), *J. Geophys. Res.*, *103*(D13), 16,369–16,383.
- Bigg, E. K., and C. Leck (2001), Properties of the aerosol over the central Arctic Ocean, *J. Geophys. Res.*, *106*(D23), 32,101–32,109.
- Birmili, W., H. Berresheim, C. Plass-Dülmer, T. Elste, S. Gilge, A. Wiedensohler, and U. Uhrner (2003), The Hohenpeissenberg aerosol formation experiment (HAFEX): A long term study including size-resolved aerosol, H₂SO₄, OH, and monoterpene measurements, *Atmos. Chem. Phys.*, *3*, 361–376.
- Bond, T., D. Streets, K. Yarber, S. Nelson, J.-H. Wo, and Z. Klimont (2004), A technology-based global inventory of black and organic carbon emissions from combustion, *J. Geophys. Res.*, *109*, D14203, doi:10.1029/2003JD003697.
- Bowling, S. A., and G. E. Shaw (1992), The thermodynamics of pollutant removal as an indicator of possible source areas for Arctic haze, *Atmos. Environ.*, *26*, 2953–2961.
- Boy, M., et al. (2005), Sulphuric acid closure and contribution to nucleation mode particle growth, *Atmos. Chem. Phys.*, *5*, 863–878.
- Bromwich, D. H., R. L. Fogt, K. I. Hodges, and J. E. Walsh (2007), A tropospheric assessment of the ERA-40, NCEP, and JRA-25 global re-analyses in the polar regions, *J. Geophys. Res.*, *112*, D10111, doi:10.1029/2006JD007859.
- Capaldo, K., P. Kasibhatla, and S. Pandis (1999), Is aerosol production within the marine boundary layer sufficient to maintain observed concentrations?, *J. Geophys. Res.*, *104*(D3), 3483–3500.
- Chin, M., D. J. Jacob, G. M. Gardner, M. S. Foreman-Fowler, P. A. Spiro, and D. L. Savoie (1996), A global three-dimensional model of tropospheric sulfate, *J. Geophys. Res.*, *101*(D13), 18,667–18,690.
- Chipperfield, M. P. (2006), New version of the TOMCAT/SIMCAT off-line chemical transport model: Intercomparison of stratospheric tracer experiments, *Q. J. R. Meteorol. Soc.*, *132*, 1179–1203.
- Christensen, J. H., et al. (2007), Regional climate projections, in *Climate Change: 2007: The Physical Science Basis. Contribution of Working Group I to the Fourth Assessment Report of the Intergovernmental Panel on Climate Change*, edited by S. Solomon et al., Cambridge University Press, Cambridge, United Kingdom and New York, NY, USA.
- Cofala, J., M. Amann, Z. Klimont, and W. Schöpp (2005), Scenarios of world anthropogenic emissions of SO₂, NO_x, and CO up to 2030, *Internal Report of the Transboundary Air Pollution Programme*, 17 pp., International Institute for Applied Systems Analysis, Laxenburg, Austria.
- Curry, J. A., W. B. Rossow, D. Randall, and J. L. Schramm (1996), Overview of Arctic cloud and radiation characteristics, *J. Clim.*, *9*, 1731–1763.
- de Gouw, J. A., A. M. Middlebrook, C. Warnake, P. D. Goldan, W. C. Kuster, J. M. Roberts, and F. C. Fehsenfeld (2005), Budget of organic carbon in a polluted atmosphere: Results from the New England Air Quality Study in 2002, *J. Geophys. Res.*, *110*, D16305, doi:10.1029/2004JD005623.
- Engvall, A.-C., R. Krejci, J. Ström, R. Treffeisen, R. Scheele, O. Hermansen, and J. Paatero (2007), Changes in aerosol properties during spring-summer period in the Arctic troposphere, *Atmos. Chem. Phys. Discuss.*, *7*, 1215–1260.
- Ferek, R. J., P. V. Hobbs, L. F. Radke, J. A. Herring, W. T. Sturges, and G. F. Cota (1995), Dimethyl sulfide in the arctic atmosphere, *J. Geophys. Res.*, *100*(D12), 26,093–26,104.
- Fiedler, V., M. Dal Maso, M. Boy, H. Aufmhoff, J. Hoffmann, T. Schuck, W. Birmili, M. Hanke, J. Uecker, F. Arnold, and M. Kulmala (2005), The contribution of sulfuric acid to atmospheric particle formation and growth: A comparison between boundary layers in Northern and Central Europe, *Atmos. Chem. Phys.*, *5*, 1773–1785.
- Gabric, A. J., B. Qu, P. Matrai, and A. C. Hirst (2005a), The simulated response of dimethylsulfide production in the Arctic Ocean to global warming, *Tellus, Ser. A and Ser. B*, *57B*, 391–403.
- Gabric, A. J., J. M. Shephard, J. M. Knight, G. Jones, and A. J. Trevana (2005b), Correlations between the satellite-derived seasonal cycles of phytoplankton biomass and aerosol optical depth in the southern ocean: Evidence for the influence of sea ice, *Global Biogeochem. Cycles*, *19*, GB4018, doi:10.1029/2005GB002546.
- Garrett, T. J., P. V. Hobbs, and L. F. Radke (2002), High Aitken nucleus concentrations above cloud tops in the Arctic, *J. Atmos. Sci.*, *59*, 779–783.
- Garrett, T. J., C. Zhao, X. Dong, G. G. Mace, and P. V. Hobbs (2004), Effects of varying aerosol regimes on low-level Arctic stratus, *Geophys. Res. Lett.*, *31*, L17105, doi:10.1029/2004GL019928.
- Generoso, S., F.-M. Bréon, F. Chevallier, Y. Balkanski, M. Schulz, and I. Bey (2007), Assimilation of POLDER aerosol optical thickness into the LMDz-INCA model: Implications for the Arctic aerosol burden, *J. Geophys. Res.*, *112*, D02311, doi:10.1029/2005JD006954.
- Giannakopoulos, C., M. P. Chipperfield, K. S. Law, and J. A. Pyle (1999), Validation and intercomparison of wet and dry deposition schemes using ²¹⁰Pb in a global three-dimensional off-line chemical transport model, *J. Geophys. Res.*, *104*(D19), 23,761–23,784.
- Guenther, A., et al. (1995), A global-model of natural volatile organic-compound emissions, *J. Geophys. Res.*, *100*(D5), 8873–8892.
- Halmer, M., H. Schmincke, and H. Graf (2002), The annual volcanic gas input into the atmosphere, in particular into the stratosphere: A global data-set for the past 100 years, *J. Volcanol. Geotherm. Res.*, *115*, 511–528.
- Heintzenberg, J., C. Leck, W. Birmili, B. Wehner, M. Tjernström, and A. Wiedensohler (2006), Aerosol number-size distributions during clear and fog periods in the summer high Arctic: 1991, 1996, and 2001, *Tellus, Ser. A and Ser. B*, *58B*, 41–50.
- Holland, M. M., C. M. Bitz, and B. Tremblay (2006), Future abrupt reductions in the summer Arctic sea ice, *Geophys. Res. Lett.*, *33*, L23503, doi:10.1029/2006GL028024.
- Intrieri, J. M., M. D. Shupe, T. Uttal, and B. J. McCarty (2002), An annual cycle of Arctic cloud characteristics observed by radar and lidar at SHEBA, *J. Geophys. Res.*, *107*(C10), 8029, doi:10.1029/2000JC000423.
- Iziomon, M. G., U. Lohmann, and P. K. Quinn (2006), Summertime pollution events in the Arctic and potential implications, *J. Geophys. Res.*, *111*, D12206, doi:10.1029/2005JD006223.
- Kawamura, K., Y. Imai, and L. A. Barrie (2005), Photochemical production and loss of organic acids in high Arctic aerosols during long-range transport and polar sunrise ozone depletion events, *Atmos. Environ.*, *39*, 599–614.
- Kerminen, V.-M., and M. Kulmala (2002), Analytical formulae connecting the “real” and “apparent” nucleation rate and the nuclei number concentration for atmospheric nucleation events, *J. Aerosol Sci.*, *33*, 609–622.
- Kettle, A. J., and M. O. Andreae (2000), Flux of dimethylsulfide from the oceans: A comparison of updated data sets and flux models, *J. Geophys. Res.*, *105*, 26,793–26,808.
- Koch, D., and J. Hansen (2005), Distant origins of Arctic black carbon: A Goddard Institute for Space Studies ModelE experiment, *J. Geophys. Res.*, *110*, D04204, doi:10.1029/2004JD005296.
- Kulmala, M., A. Laaksonen, and L. Pirjola (1998), Parameterizations for sulfuric acid/water nucleation rates, *J. Geophys. Res.*, *103*(D7), 8301–8307.
- Kulmala, M., H. Vehkamäki, T. Petäjä, M. Dal Maso, A. Lauri, V.-M. Kerminen, W. Birmili, and P. H. McMurry (2004), Formation and growth rates of ultrafine atmospheric particles: A review of observations, *J. Aerosol Sci.*, *35*, 143–176.
- Kulmala, M., K. E. J. Lehtinen, and A. Laaksonen (2006), Cluster activation theory as an explanation of the linear dependence between formation rate of 3 nm particles and sulfuric acid concentration, *Atmos. Chem. Phys.*, *6*, 787–793.
- Law, K. S., and A. Stohl (2007), Arctic air pollution: Origins and impacts, *Science*, *315*, 1537–1540.
- Lawson, R. P., B. A. Baker, C. G. Schmitt, and T. L. Jensen (2001), An overview of microphysical properties of Arctic clouds observed in May and July 1998 during FIRE ACE, *J. Geophys. Res.*, *106*(D14), 14,989–15,014.
- Leck, C., and E. K. Bigg (2005a), Source and evolution of the marine aerosol—A new perspective, *Geophys. Res. Lett.*, *32*, L19803, doi:10.1029/2005GL023651.
- Leck, C., and E. K. Bigg (2005b), Biogenic particles in the surface micro-layer and overlying atmosphere in the central Arctic Ocean during summer, *Tellus, Ser. A and Ser. B*, *57B*, 305–316.

- Lubin, D., and A. M. Vogelmann (2006), A climatologically significant aerosol longwave indirect effect in the Arctic, *Nature*, *439*, 453–456.
- Lubin, D., and A. M. Vogelmann (2007), Expected magnitude of the aerosol shortwave indirect effect in springtime Arctic liquid water clouds, *Geophys. Res. Lett.*, *34*, L11801, doi:10.1029/2006GL028750.
- Mårtensson, M., D. Nilsson, G. de Leeuw, L. H. Cohen, and H.-C. Hansson (2003), Laboratory simulations and parameterization of the primary marine aerosol production, *J. Geophys. Res.*, *108*(D9), 4297, doi:10.1029/2002JD002263.
- Middlebrook, A. M., D. M. Murphy, and D. S. Thomson (1998), Observations of organic material in individual marine particles at Cape Grim during the first Aerosol Characterization Experiment (ACE 1), *J. Geophys. Res.*, *103*(D13), 16,475–16,484.
- Monahan, E., D. Spiel, and K. Davidson (1986), A model of marine aerosol generation via whitecaps and wave disruption, in *Oceanic Whitecaps and Their Role in Air-Sea Exchange Processes*, edited by E. C. Monahan and G. MacNiocaill, pp. 167–174, D. Reidel Publishing, Dordrecht.
- Nenes, A., and J. Seinfeld (2003), Parameterization of cloud droplet formation in global climate models, *J. Geophys. Res.*, *108*(D14), 4415, doi:10.1029/2002JD002911.
- Nenes, A., S. Ghan, H. Abdul-Razzak, P. Y. Chuang, and J. Seinfeld (2001), Kinetic limitations on cloud droplet formation and impact on cloud albedo, *Tellus, Ser. A and Ser. B*, *53B*, 133–149.
- Nightingale, P. D., G. Malin, C. S. Law, A. J. Watson, P. S. Liss, M. I. Liddicoat, J. Boutin, and R. C. Upstill-Goddard (2000), In situ evaluation of air-sea gas exchange parameterizations using novel conservative and volatile tracers, *Global Biogeochem. Cycles*, *14*, 373–388.
- Nilsson, E. D., Ü. Rannik, E. Swietlicki, C. Leck, P. P. Aalto, J. Zhou, and M. Norman (2001), Turbulent aerosol fluxes over the Arctic Ocean. 2. Wind-driven sources from the sea, *J. Geophys. Res.*, *106*(D23), 32,139–32,154.
- Quinn, P. K., T. L. Miller, T. S. Bates, J. A. Ogren, E. Andrews, and G. E. Shaw (2002), A 3-year record of simultaneously measured aerosol chemical and optical properties at Barrow, Alaska, *J. Geophys. Res.*, *107*(D11), 4130, doi:10.1029/2001JD001248.
- Quinn, P. K., G. Shaw, E. Andrews, E. G. Dutton, T. Ruoho-Airola, and S. L. Gong (2007), Arctic haze: Current trends and knowledge gaps, *Tellus, Ser. A and Ser. B*, *59B*, 99–114.
- Raatz, W. E., and G. E. Shaw (1984), Long-range transport of pollution aerosols into the Alaskan Arctic, *J. Clim. Appl. Meteorol.*, *23*, 1052–1064.
- Raes, F. (1995), Entrainment of free tropospheric aerosols as a regulating mechanism for cloud condensation nuclei in the remote marine boundary layer, *J. Geophys. Res.*, *100*(D2), 2893–2903.
- Rasch, P. J., et al. (2000), A comparison of scavenging and deposition processes in global models: Results from the WCRP Cambridge Workshop of 1995, *Tellus, Ser. A and Ser. B*, *52B*, 1025–1056.
- Raymond, T., and S. Pandis (2002), Cloud activation of single-component organic aerosol particles, *J. Geophys. Res.*, *107*(D24), 4787, doi:10.1029/2002JD002159.
- Rinke, A., K. Dethloff, and M. Fortmann (2004), Regional climate effects by Arctic haze, *Geophys. Res. Lett.*, *31*, L16202, doi:10.1029/2004GL020318.
- Rotstajn, L. D., and U. Lohmann (2002), Simulation of the tropospheric sulfur cycle in a global model with a physically based cloud scheme, *J. Geophys. Res.*, *107*(D21), 4592, doi:10.1029/2002JD002128.
- Seland, Ø., and T. Iversen (1999), A scheme for black carbon and sulphate aerosols tested in a hemisphere scale, Eulerian dispersion model, *Atmos. Environ.*, *33*, 2853–2879.
- Sellegrì, K., C. D. O'Dowd, Y. J. Yoon, S. G. Jennings, and G. de Leeuw (2006), Surfactants and submicron sea spray generation, *J. Geophys. Res.*, *111*, D22215, doi:10.1029/2005JD006658.
- Shaw, G. E. (1984), Microparticle size spectrum of Arctic haze, *Geophys. Res. Lett.*, *11*(5), 409–412.
- Shaw, G. E. (1995), The Arctic haze phenomenon, *Bull. Am. Meteorol. Soc.*, *76*, 2403–2413.
- Sihto, S.-L., et al. (2006), Atmospheric sulphuric acid and aerosol formation: Implications from atmospheric measurements for nucleation and early growth mechanisms, *Atmos. Chem. Phys.*, *6*, 4079–4091.
- Spracklen, D., K. Pringle, K. Carslaw, M. Chipperfield, and G. Mann (2005a), A global off-line model of size-resolved aerosol microphysics: I. Model development and prediction of aerosol properties, *Atmos. Chem. Phys.*, *5*, 2227–2252.
- Spracklen, D., K. Pringle, K. Carslaw, M. Chipperfield, and G. Mann (2005b), A global off-line model of size-resolved aerosol microphysics: II. Identification of key uncertainties, *Atmos. Chem. Phys.*, *5*, 3233–3250.
- Spracklen, D., K. Carslaw, M. Kulmala, V.-M. Kerminen, G. Mann, and S.-L. Sihto (2006), The contribution of boundary layer nucleation events to total particle concentrations on regional and global scales, *Atmos. Phys. Chem.*, *6*, 5631–5648.
- Spracklen, D., K. Pringle, K. Carslaw, G. Mann, P. Manktelow, and J. Heintzenberg (2007), Evaluation of a global aerosol microphysics model against size-resolved particle statistics in the marine atmosphere, *Atmos. Chem. Phys.*, *7*, 2073–2090.
- Stier, P., et al. (2005), The aerosol-climate model ECHAM5-HAM, *Atmos. Chem. Phys.*, *5*, 1125–1165.
- Stockwell, D., and M. Chipperfield (1999), A tropospheric chemical-transport model: Development and validation of the model transport schemes, *Q. J. R. Meteorol. Soc.*, *125*, 1747–1783.
- Stohl, A. (2006), Characteristics of atmospheric transport into the Arctic troposphere, *J. Geophys. Res.*, *111*, D11306, doi:10.1029/2005JD006888.
- Stohl, A., et al. (2006), Pan-Arctic enhancements of light absorbing aerosol concentrations due to North American boreal forest fires during summer 2004, *J. Geophys. Res.*, *111*, D22214, doi:10.1029/2006JD007216.
- Ström, J., J. Umegård, K. Tørseth, P. Tunved, H.-C. Hansson, K. Holmén, V. Wisnann, A. Herver, and G. König-Langlo (2003), One year of particle size distribution and aerosol chemical composition measurements at the Zeppelin station, Svalbard, March 2000–2001., *Phys. Chem. Earth*, *28*, 1181–1190.
- Tervahattu, H., J. Juhanoja, and K. Kupiainen (2002), Identification of an organic coating on marine aerosol particles by TOF-SIMS, *J. Geophys. Res.*, *107*(D16), 4319, doi:10.1029/2001JD001403.
- Tjernström, M. (2005), The summer Arctic boundary layer during the Arctic Ocean Experiment 2001 (AEO-2001), *Boundary Layer Meteorol.*, *117*, 5–36.
- Trevena, A. J., G. B. Jones, S. W. Wright, and R. L. van den Enden (2000), Profiles of DMSP, algal pigments, nutrients and salinity in pack ice from eastern Antarctica, *J. Sea Res.*, *43*, 265–273.
- Turner, S. M., P. D. Nightingale, W. Broadgate, and P. S. Liss (1995), The distribution of dimethyl sulphide and dimethylsulphoniopropionate in Antarctic waters and sea ice, *Deep Sea Res., Part II*, *42*, 1059–1080.
- van der Werf, G. R., J. T. Randerson, G. J. Collatz, and L. Giglio (2003), Carbon emissions from fires in tropical and subtropical ecosystems, *Global Change Biol.*, *9*, 547–562.
- Weber, R. J., J. J. Marti, P. H. McMurry, F. L. Eisele, D. J. Tanner, and A. Jefferson (1996), Measured atmospheric new particle formation rates: Implications for nucleation mechanisms, *Chem. Eng. Commun.*, *151*, 53–64.
- Wiedensohler, A., D. S. Covert, E. Swietlicki, P. Aalto, J. Heintzenberg, and C. Leck (1996), Occurrence of an ultrafine particle mode less than 20 nm in diameter in the marine boundary layer during Arctic summer and autumn, *Tellus, Ser. A and Ser. B*, *48B*, 213–222.
- Xie, Z., J. D. Blum, S. Utsunomiya, R. C. Ewing, X. Wang, and L. Sun (2007), Summertime carbonaceous aerosols collected in the marine boundary layer of the Arctic Ocean, *J. Geophys. Res.*, *112*, D02306, doi:10.1029/2006JD007247.
- Yamanouchi, T., et al. (2005), Arctic Study of Tropospheric Aerosol and Radiation (ASTAR) 2000: Arctic haze case study, *Tellus, Ser. A and Ser. B*, *57B*, 141–152.

K. S. Carslaw, H. Korhonen, D. A. Ridley, and D. V. Spracklen, School of Earth and Environment, University of Leeds, Leeds LS2 9JT, UK. (hannele.korhonen@uku.fi)

J. Ström, Department of Applied Environmental Science, University of Stockholm, Stockholm S10691, Sweden.